Vol. 6 Oct. 2009

AUTOMOTIVE COMPILATION

EDITORIAL

Welcome to our sixth edition of Automotive Compilation! As the previous issues, it presents a range of articles focusing on Atmel's technologies and products. Application hints aim to support designers to create innovative system solutions for the ever-evolving automotive industry.

Modern cars contain 70plus Electronic Control Units (ECUs), and the amount of electronics in cars will continue to increase significantly in the future. By 2015, the amount of electronics is projected to be about 40% of the value of a car. The increased complexity of these systems requires microcontrollers with high calculation performance. The first article in this edition discusses why a high-throughput 32-bit microcontroller architecture such as the AVR32 is required to address tomorrow's automotive challenges.

Following the article on electric and hybrid vehicles in issue 5, the article "New Li-Ion Battery Management Chipset" describes Atmel's new battery management and monitoring devices in more detail.

Passive Entry (PE) systems set a new trend for automotive comfort and security. Although they were available already years ago, they have become more popular recently as their increased integration level allows for lower system costs. The article "RF Design Considerations" provides system designers useful hints how to set-up a PES system, while "Predicting RF Range Performance" focuses on the physics of electro-magnetic wave behavior and its behavior in a real-world environment.

Brushless motors are becoming increasingly important in the automotive area, since the advantages are obvious. BLDC motors are already used in fuel pumps, steering systems and fan controllers for air conditioning systems. The quietness of these motors allows them to be used in convenience applications in vehicle interiors, such as power windows and air conditioning flap controllers. The article describes both the principles of such a BLDC motor control solution and also the functionality of Atmel's BLDC devices.

Another focus area is LIN networking. The expected increase in the amount of LIN devices in the coming years can be explained by the continued requirement for comfort functions in next-generation automotives. As almost all comfort functions can be controlled by the passengers via keypads, it is expected that the amount of the keypads will also increase. Therefore, we examine efficient keypad evaluation using a switch matrix module. Another article explains LIN Node Mirror Positioning and Folding.

We hope you enjoy our sixth installment of Atmel's Automotive Compilation.

Dr. Matthias Kästner
Senior Director Marketing
RF & Automotive Business Unit

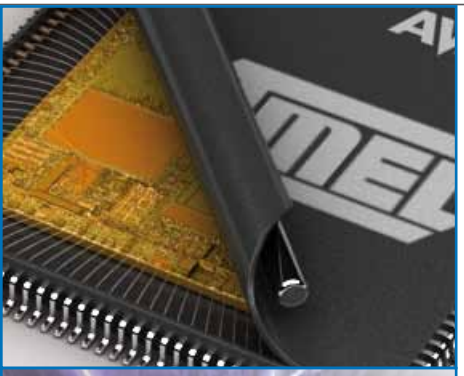

STANDARD PRODUCTS

SECURITY

Car Infotainment

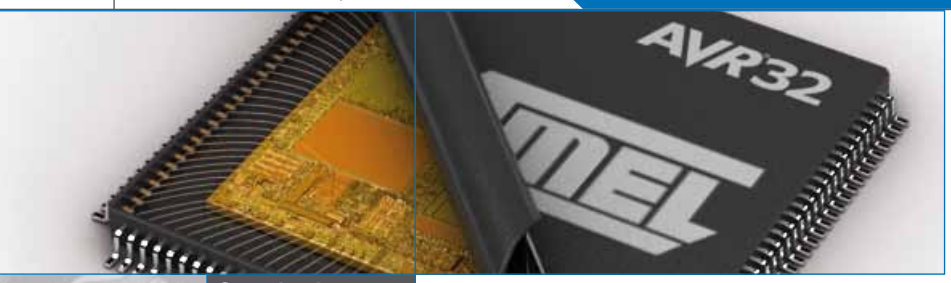

Standard Products

Networking

LIN

AVR32: High-throughput 32-bit Microcontroller Architecture Addresses Tomorrow's Automotive Challenges

Detlef Schick

The car industry has gone a long way since its beginning. Modern cars contain 70plus Electronic Control Units (ECUs), and the amount of electronics in cars will continue to increase significantly in the future. By 2015 the amount of electronics is projected to be about 40% of the value of a car.

Electronics is the key enabler of today's innovations in the automotive industry. There is a virtually unlimited amount of possibilities how electronics can be used in future cars. The integration of multimedia systems allow the driver to stay focused. Active safety systems and driver assistant systems such as ESP, tire pressure monitoring, adaptive cruise control, lane departure warning or pre-crash systems improve the safety and help to achieve 2001's target to cut the amount of fatal accidents in the EU in half by 2010.

Political aspects such as the European-wide reduction of the CO_2 emissions are also reason for an increased demand of semiconductors in cars. No matter if it is called Efficient Dynamics, Blue Efficiency, Blue Motion or whatever name the OEM have given their system – they all use smart electronics to reduce the gas consumption of their cars. Start-Stop systems require battery monitoring and voltage stabilization with DC-DC converters. Demand-driven power steering and power brakes use BLDC motor controls, just to name a few of them.

The increased complexity of these systems requires microcontrollers with high calculation performance. As complex systems are more vulnerable to errors a great deal of diagnosis functions is implemented in software. Additional performance is required to ensure that the diagnosis can be executed simultaneously without influencing the application negatively. The standardization of software via Autosar is driven by all major OEM and will also increase the software overhead significantly.

Why Using an AVR32 Microcontroller?

This brings us back to the initial question of why a high-throughput 32-bit microcontroller architecture such as the AVR®32 is required to address tomorrow's automotive challenges. Why can't designers just:

1. Increase the clock speed of the controller?
2. Add coprocessors or use dual/multiple cores?

This could be done, of course, but will it be the optimal solution? As the power dissipation increases linear with the clock speed, the current consumption in active mode will be twice as high if the clock speed is doubled. This might not be a big issue if the engine of the car is running but if the part lives on

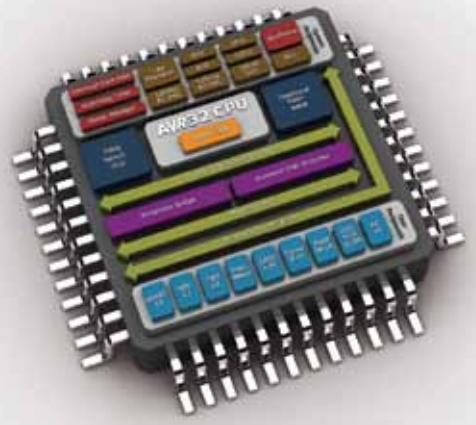

a tight power budget, e.g., when it wakes up from sleep mode to check the status of a sensor, this is a different story. As each process technology has its speed limitations an increase of the processor clock quite often requires to use a smaller process geometry. This, however, means an increase of the leakage currents and thus a higher current consumption in sleep mode. Semiconductors of smaller process geometries are more susceptible to “soft errors” in their memory which are caused by Neutrons and Alpha Radiation. As the internal signal levels are decreased with each process shrink the parts are also more susceptible to electromagnetic fields.

Adding a coprocessor or dual/multiple core is something which will be seen more and more in the automotive industry. For safety-critical systems this might be mandatory due to supervisor or redundancy constraints. It also makes sense for high-performance systems to limit the current consumption and heat dissipation. For specific applications, Atmel will also provide multi-core solutions.

But this is not a general solution to overcome architectural weaknesses – although it is, unfortunately, still common practice to boost the performance of 8-bit, 16-bit and also weak 32-bit microcontrollers. Silicon costs are generally higher if multiple cores have to be implemented. And if the costs are optimized, designers will end up in most cases with a part which is just usable for one specific purpose. Another disadvantage of coprocessor- or multi-core systems is the increased complexity of the software development.

The automotive market has three fundamental requirements in perspective to future controllers. Firstly, microcontrollers must have a low current consumption to preserve the battery if the car is parked but also to reduce the current consumption and the related CO_2 consumption. Secondly, these controllers need to provide a high calculation performance under the described constraints. And third, the controller architecture has to comply with future safety trends such as ISO26262.

The AVR32 architecture with its exceptionally high throughput was designed to address all three requirements. Atmel's UC3 family of Flash-based microcontrollers offers up to 91 DMIPS at 66 MHz clock speed which outperforms all competing architectures in this class of controllers. The innovative architecture was designed by Atmel engineers, and 19 patents have been filed. Some architectural highlights are described in the following.

Instruction Set Architecture (ISA)

The Instruction Set Architecture (ISA) of the AVR32 UC core has over 220 instructions available as **16-bit compact and 32-bit extended instructions** which are freely intermixable. It is designed to minimize the code size and data transactions between the core and memories, which saves both power and CPU clock cycles. The compiler automatically selects the most efficient compact or extended form of each instruction, providing the user the fastest and most efficient code possible. The integrated **DSP extensions** such as, e.g., single-cycle multiply accumulate instructions make this architecture particularly suited for calculation-intensive applications (such as digital filtering, FFT, decoding or decompression of data).

In many applications, such as networked applications, it is important to efficiently extract bit fields from a register, or insert bit fields into a register for data packet handling. The AVR32 ISA includes **bit field instructions** such as bit field insertion and zero- or sign-extended extraction. These instructions execute in one clock cycle only which is radically faster than most conventional architectures that rely on a sequence of shifts and logical operations to perform the same function.

Microcontrollers wouldn’t be what they are if it would not be for their

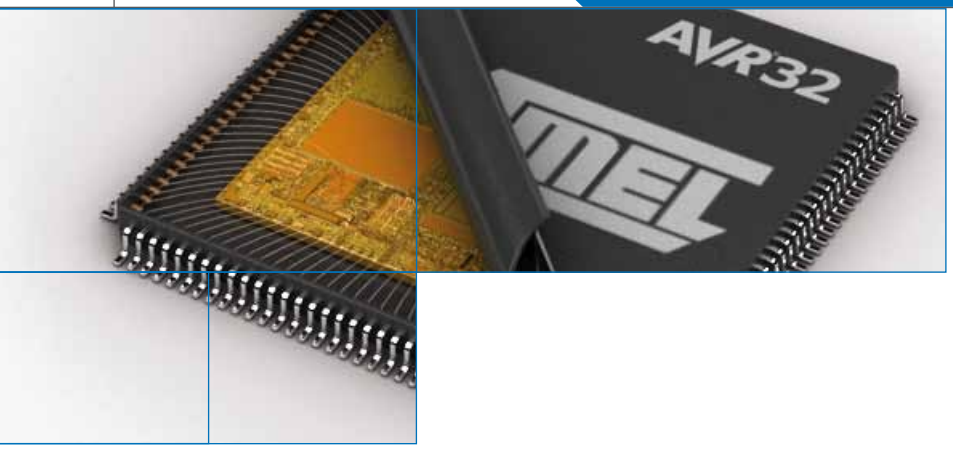

controlling abilities. This requires efficient bit manipulation of the internal configuration registers which typically consist of a multiple instruction sequence: read the corresponding register – change the relevant value using logical operators like OR and AND – write the updated value back to the register. The AVR32 instruction set includes **atomic Read-Modify-Write instructions** which perform all three instructions in one single cycle instruction: bit set, bit clear and bit toggle for any memory location. These are performed by the memc, mems and memt instructions.

The AVR32 UC code is consistently 5% to 20% smaller than code compiled for the ARM® Thumb® instruction set. More significantly, when code is optimized for execution speed, the AVR32 UC code is 30% to 50% more compact than code compiled for the ARM instruction set. Executing a Fast Fourier Transformation (FFT) shows a 40% performance gain of the UC3 compared to a comparable part based on ARM's new innovation, their CoretexM3 architecture.

3-stage Single-cycle Pipeline

The 3-stage single-cycle pipeline of the AVR32 UC core is optimized for real-time applications. It does not contain a super scalar pipeline as with the AVR32 AP7 architecture, which comes with instruction and data caches, data forwarding, hazard detection or branch prediction. Instead the UC3 architecture has a pipeline which is optimized for a fast execution speed with a deterministic timing behavior. The first pipeline stage pre-fetches one 32-bit or two 16-bit instructions every clock cycle into an internal instruction buffer. The buffer ensures that the pipeline completely prevents pipeline stalls during sequential program execution. Execution from on-chip Flash can be sustained at the maximum CPU clock frequency without the CPU having to stall waiting for instructions from the Flash. The second stage decodes instructions and generates necessary signals for instruction execution. The third stage is made of three execution sub-units: the ALU, multiplication, and load/store units. The ALU performs arithmetical and logical operations, including hardware division. The multiply unit executes the numerous multiply and multiply-and-accumulate (MAC) operations available from the instruction set architecture (ISA), and the load/store unit performs single-cycle memory accesses to SRAM or accesses on the high-speed bus (HSB). There are no data hazards in the AVR32 UC core so the register files can be updated during the same clock cycle as the instruction is executed. This makes assembly programming simpler compared to deeper pipelines as no code scheduling is needed.

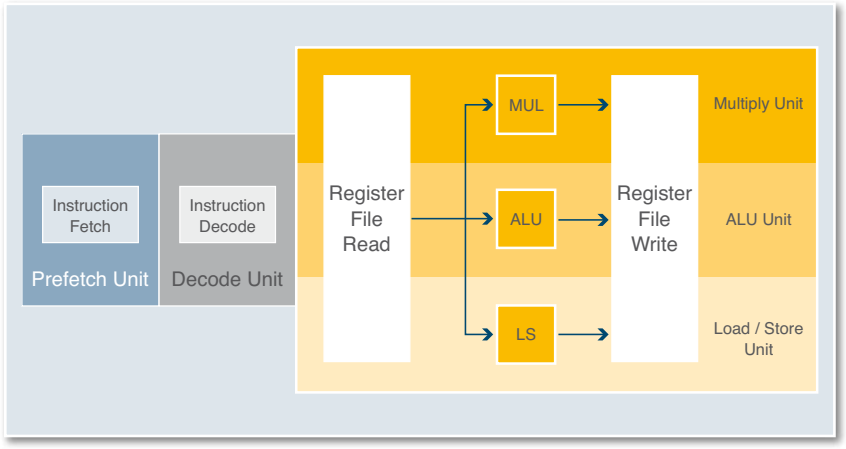

Figure 1. The 3-stage Single-cycle Pipeline with the Three Execution Sub Units of the Third Stage

Peripheral DMA Controller

Data-intensive applications such as networking applications, with streams of data passing between the peripherals and the memories, can seriously compromise the CPU. The on-chip multi-channel peripheral DMA controller provides tight integration of peripherals and memory, and is directly mapped into the programming memory of each peripheral. Without DMA a simple SPI communication will load the CPU with 17.7% at 400 kBit and with 53.4% at 1.2 MBit. The DMA of the UC3 architecture, however, offloads the CPU to a level of only 0.4% load at 400 kBit and 1.2% at 1.2 MBit. Using the DMA in combination with the ADC allows to autonomously store ADC measurements in a predefined memory area for the CPU to analyze the acquired data in due time. This can be done while the CPU is in sleep mode which can significantly reduce the power consumption as the core can stay in sleep mode during the acquisition phase.

Multi-layer Bus Architecture with Dynamic Frequency Scaling

Instead of only implementing the two busses for instruction and data fetch which comprise a Harvard architecture, the Atmel engineers implemented an entire bus matrix. This ensures that the peripherals can operate independent from each other / the CPU, eliminating the wait states with are typically required in a system with a shared bus. The multi-layer bus architecture with dynamic frequency scaling interconnects up to 16 High Speed Bus (HSB) masters to up to 16 HSB slaves. Current UC3 products include up to 8 individual bus layers. Different types of peripherals require different bus frequencies. For example, SPI and UART can get by with a substantially lower clock than a CAN, 10/100 Ethernet MAC or high-speed USB. In a conventional multi-layer bus structure, the fastest peripheral will dictate the clock frequency of the entire bus. The UC3's peripherals are connected through three individual bus bridges (Bridge A to C) which can run at individual clock speeds. Minimizing the speed of each of these three clock domains as well as the speed of the CPU and Matrix helps to optimize the system's current consumption.

Integrated Single-cycle Read/Write SRAM

The AVR32 UC core is the industry's first core with integrated single-cycle read/write SRAM as part of the core itself. It has a direct interface to the CPU that bypasses the system bus to achieve faster execution, cycle determinism and lower power consumption. Conventional microcontroller architectures require one extra clock cycle as the SRAM is connected to the main bus which requires one clock cycle to output the address and a second one to

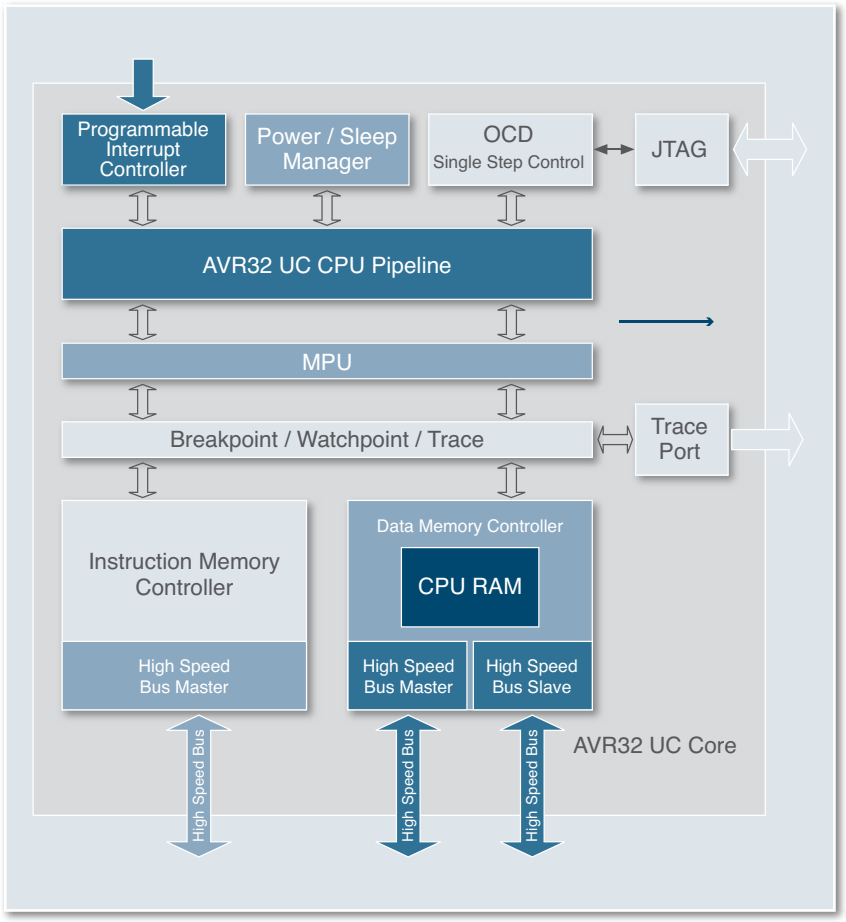

Figure 2. UC3 Core Block Diagram with Tightly Coupled CPU SRAM Ensuring Single-cycle Memory Access

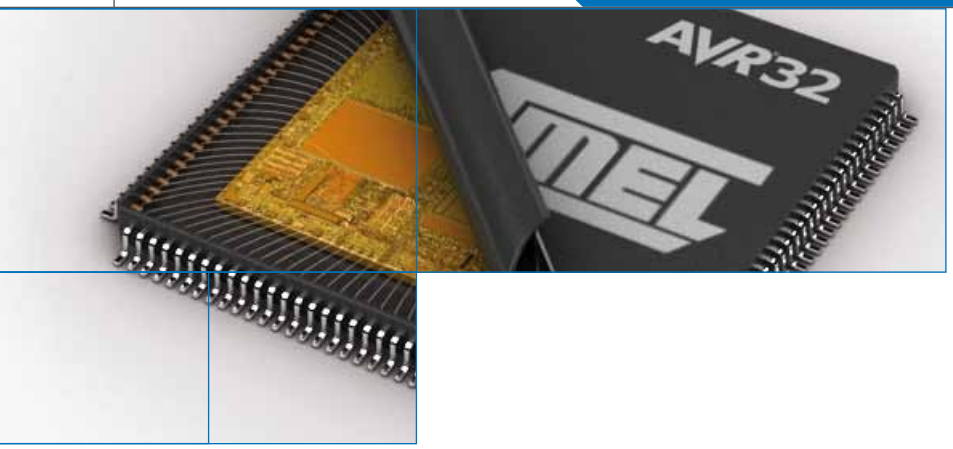

read/write the data. An HSB slave interface access allows DMA controllers or other HSB masters to write to or read data directly from the closely coupled SRAM. Arbitration is performed if the CPU and a high-speed slave request access simultaneously. The priority scheme is programmable to suit different application needs.

Interrupt Controller

The UC3's interrupt controller has 64 groups of interrupts (each with an individual autovector) and 4 different interrupt priority levels. In combination with the Non-Maskable Interrupt (NMI) this ensures a fast and deterministic interrupt response and makes this part well suited for the usage of operating systems. Pending events of a higher priority class may preempt handling of on-going events of a lower priority class. The CPU is also able to abort multi-cycle instructions if interrupt requests are pending during more than 5 clock cycles, limiting the maximum interrupt latency to 16 cycles maximum.

When an interrupt is accepted, eight registers are automatically stored to stack. The execution of the interrupt handler routine then continues from the address which

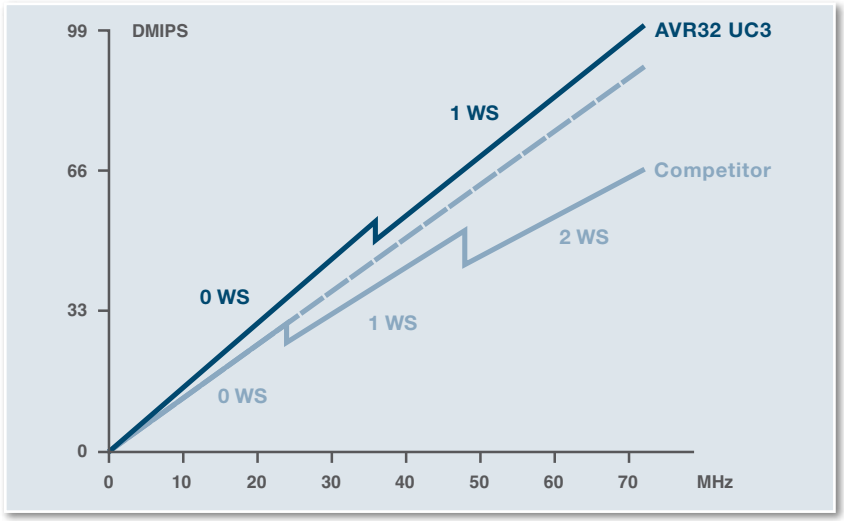

Figure 3. With Increasing CPU Speeds the Fewer Wait State in the Flash Memory Access Accelerate the Performance Gain of the UC3 Compared to Completing Architectures.

is specified by the autovector. When resuming from the interrupt handler, previously saved registers are automatically popped from the system stack before carrying out the next instruction from the main instruction flow.

Flash Performance

The program is stored in the microcontroller's on-chip Flash memory and it is directly executed from there. The Flash performance thus significantly influences the overall performance of the controller. Since the Flash read-time is too slow at higher CPU speeds to support reading one instruction each CPU clock cycle, all 32-bit Flash microcontrollers introduce wait cycles in their Flash access. Program caches and the UC3's 16-bit instructions help to reduce this effect to a minimum. In combination with the fast Flash function, this results in fewer wait cycles than with competitive solutions.

Memory Protection Unit

Operating systems for safety-critical applications such as OSEK-compliant OS for the automotive industry require the usage of a control-

ler with a Memory Protection Unit (MPU). The complexity of today's applications is typically distributed on multiple tasks which run in parallel. While task scheduling is done by the OS, the MPU controls the access to the memory and prevents any unpermitted memory accesses. If a protected memory location is accessed without authorization, an exception is executed. Atmel's latest UC3 devices incorporate a Secure Access Unit (SAU) together with the MPU. The MPU is set up to protect chunks of memory while the SAU provides a secure channel into specific memory locations that are protected by the MPU. This gives more flexibility and faster access to protected areas.

Floating Point Unit

Another architectural feature driven by the automotive industry is the 32-bit Floating Point Unit (FPU). An FPU provides numerous advantages, one of which is the increased floating point operations accuracy. Model-based application design and simulation is widely used in today's designs. Tools such as Matlab and Simulink from MathWorks are used for complex modeling and simulation; and they use floating point values. A reduction to fixed point numbers is possible in some cases but this introduces errors that require a thorough analysis. With the UC3's on-chip FPU this can be avoided without performance penalty.

Conclusion

The compact code as a result of the powerful and innovative instruction set leaves less instructions to execute than with comparable architectures. The directly coupled SRAM and the optimized 3-stage pipeline both eliminate wait states and ensure a seamless and fast code execution. The multi-layer bus structure in combination with the DMA functionality offloads the CPU and allows parallel data processing. Additional instruction cycles are saved as the efficient interrupt and exception handler allows fast task switches and interrupt execution.
The combination of these innovations have made the AVR32 to what it is, and are the basis of its exceptional high throughput. Atmel's process technologies are one reason for its leadership in low-power microcontrollers. True low-power devices, however, also need to be high-throughput devices since only a high throughput allows to reduce the number of power-consuming memory accesses to a minimum. Lowering the CPU clock speed goes along with a reduction of the corresponding current consumption.

The UC3's current consumption is minimal, but even enables further reduction since the two separate peripheral bus bridges allow different clock frequencies to be set for high- and low-speed peripherals. This means slower peripherals can operate on a slower bus that draws less power.

Atmel's UC3 portfolio is rapidly expanding and currently consists of six sub-families, each with a peripheral set optimized for specific market segments. The next edition or the Automotive Compilation will cover the powerful peripheral set and how an individual application can benefit from its innovative features.

Standard Products

New Li-Ion Battery Management Chipset ATA6870, ATA6871 for Electrical and Hybrid Vehicles

Claus Mochel

Electric or hybrid vehicles offer a viable means of increasing the efficiency of today's cars and thus tackling the dual problems of fuel consumption and CO_2 emissions. At the heart of electric or hybrid engines is a powerful battery; however, the amount of storable energy in these vehicles is limited by the weight and mass of the battery. New generations of Lithium Ion (Li-Ion) batteries are up to 30% smaller and 50% lighter than conventional Nickel Metal Hybrid (NiMH) batteries. These Li-Ion batteries offer concrete advantages in terms of size, weight, recharge speed, life span, and resistance to memory effects.

For this reason, the majority of electric and hybrid vehicle manufacturers have now started to develop high-performance batteries on a Li-Ion basis. This is no easy task because these high-performance batteries are energy bundles that provide voltages of between 150V and 500V, and even up to 1000V or more for busses. These high voltages are needed for an extremely simple reason. With a voltage of 1V, 1000A of current would be needed to generate 10 kW of output with an electric drive. In this case just a few mΩ of line resistance would prevent any energy whatsoever from reaching the motor because of the voltage drop caused by the current. However, with a voltage of 500V, only 20A would be needed into provide the same output.

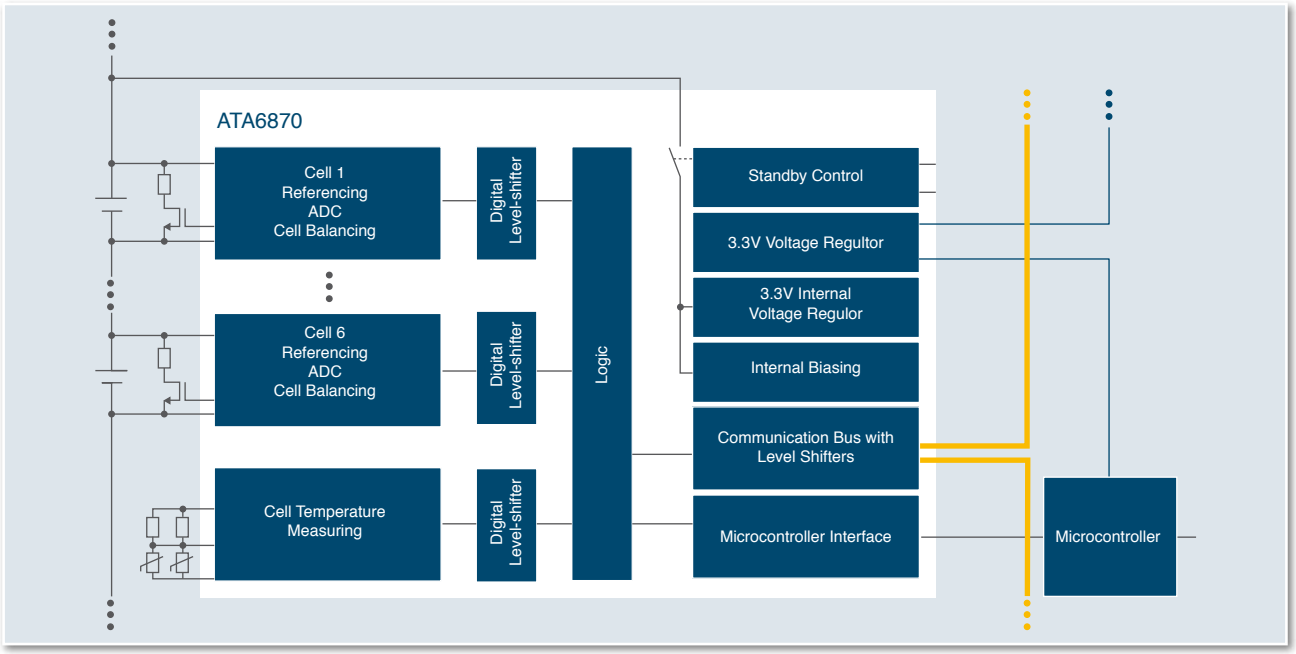

Figure 1. Block Diagram Battery Management Circuit

In order to provide these high voltages, approximately 50-200 cells with a typical cell voltage of approx. 3.6V are connected in series in several strings. Each individual cell is electronically monitored so that functions such as state-of-charge determination, cell balancing, overvoltage/undervoltage monitoring and temperature monitoring can be provided. In order to make this monitoring as simple as possible, Atmel has developed the ATA6870, a measuring, power supply and cell balancing circuit for Li-Ion batteries.

ATA6870, Measuring, Power Supply and Charge Balancing IC

In addition to 6 high-precision AD converters for cell voltage measurement, the ATA6870 also features charge balancing between the individual cells. The capacity of battery cells varies due to the manufacturing process, self-discharging and ageing. Charge balancing is carried out between the individual cells so that the performance of the entire battery is not determined by the weakest cell. This is done by using a bypass switch to make the energy bypass a cell via a resistor and go to the next one. In order to prevent the balancing from taking a long time because of the large number of cells in a modern high-performance battery, the charge balancing can be carried out simultaneously at any number of cells in the ATA6870.

The heart of the ATA6870, however, are the high-precision 12-bit AD converters. Each cell is monitored by its own AD converter. This allows all cells to be measured at the same time, which is important for the state-of-charge detection of a complete battery. Moreover, the cell voltage does not need to be analog-level-shifted to the IC's ground potential, which would decrease the converter accuracy. The ATA6870 shifts the digital result of the ADC without any accuracy losses. This is crucial as the AD converter accuracy is one of the most important features of a Li-Ion battery management IC. However, it is no use having high precision if the DC signal that is being measured is superimposed with noise or spikes, which are unavoidable with the high currents and load changes of a battery. For this reason the ATA6870 has an incremental AD converter. During the sampling time of 8.2 ms, this automatically forms the average of the signal that is present at the input. Noise and voltage spikes are therefore reliably suppressed. This also impressively demonstrates the filtering characteristics of the AD converter (see figure 2), a low pass with an extremely low cut-off frequency of 30 Hz.

However, the biggest impression is made by the "no-drift" reference voltage that is used in the AD converter, which is not influenced at all by temperature (see figure 3). As well as the basic functions of a battery management IC such as

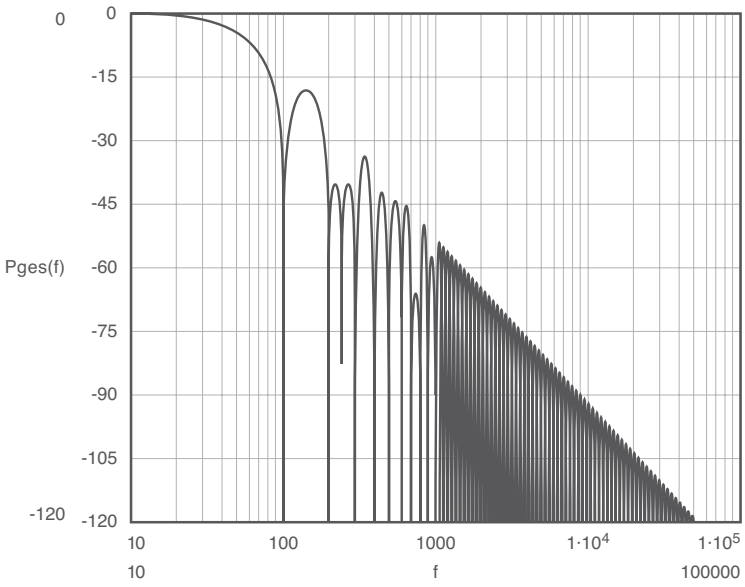

Figure 2. Input Filter for Cell-voltage Measurement

cell voltage measurement, cell temperature measurement and charge balancing, the ATA6870 also has a multitude of other characteristics. One of these is known as “hot plug-in capability”, a feature that is extremely important in the battery manufacturing process. When the modules containing the monitoring electronics are connected to the battery cells during the manufacturing process, they are already at their full voltage. Because of the large number of cells that are connected in series, it is not impossible for individual IC inputs to be subjected to overvoltage for short periods or even have reverse polarity because of timing during assembly or by the contact bouncing that occurs when they are being plugged together. It goes without saying that the battery management IC must not be destroyed in this case. Another reliability feature is the extremely robust data communication between the stacked ICs, which is based on current sources. This data transmission can be made even more reliable if the user activates the checksum feature. This is an 8-bit security code which is generated from the transferred data and then appended to it.

A battery management system also needs a microcontroller, which, in turn, requires a voltage supply. To avoid that the microcontroller’s power consumption causes any cell imbalance, the controller that generates the supply voltage must obtain its power from the highest cell in the string, and lead it back via the lowest cell. This means, of course, that several 100V of voltage will be lost via this controller in extreme cases. The ATA6870 solves this issue by providing the option to stack the integrated power supply for the microcontroller to the IC itself. Thus, the current that is needed to supply the microcontroller can be taken from the top cell, and be fed back into the battery string’s bottom cell. This helps designers to save expensive high-voltage devices.

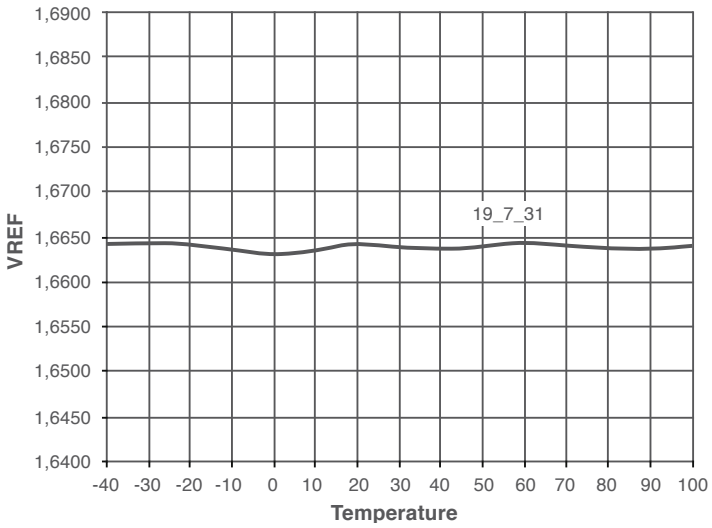

Figure 3. ADC Reference-voltage Temperature Characteristic

ATA6871 Secondary Li-Ion Battery Protection Device

Unfortunately, Li-Ion batteries also feature some undesirable characteristics. In case of overcharging or deep discharging they tend to heat or – in some exceptional cases – to burn. To prevent this, a special safety concept is necessary. Atmel uses a 2-chip strategy that ensures a continuously operating security mechanism, even in the event of device destruction due to, for example, overvoltage.

As previously explained, the ATA6870 operates as a precise cell voltage and overtemperature monitoring circuit. The ATA6871 (which can be stacked the same way as the ATA6870) serves as second-

ary protection device and provides additional security if the ATA6870 fails due to software errors or destruction. The ATA6871 monitors 6 Li-Ion cells via comparators with regard to over- and undervoltage. An additional comparator for temperature monitoring is optionally available. The device incorporates a hardware-implemented self test that checks the circuit's functions: over- and undervoltage, cell temperature, and data communication between the ICs. In addition, the cables to the battery cells are monitored to prevent disconnection or short-circuit. This is done without using a microcontroller, thus avoiding any potential software errors. By doing so, the ATA6871 sets completely new benchmarks for safe Li-Ion battery monitoring.

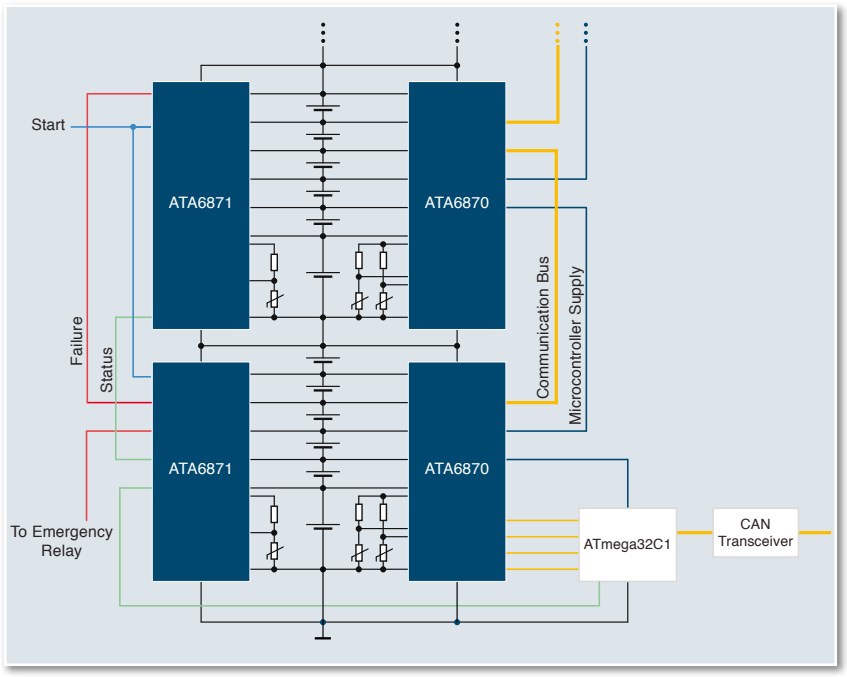

Figure 4. Primary / Secondary Protection System Overview

Evaluation Kit

Atmel supplies evaluation boards for the two ATA6870 and ATA6871 battery monitoring circuits that enable customers to test the components easily and quickly. On each of these boards there are three ATA6870s or ATA6871s in a stack for monitoring the 18 Li-Ion battery cells. Of course, the boards are stackable, meaning that a complete monitoring system for a Li-Ion high-performance battery can be quickly and easily set up in the laboratory and evaluated.

For the ATA6870 Atmel also provides actuation software with a graphical user interface that allows the boards to be easily controlled from a PC or laptop. As well as measuring and providing a graphical display of the cell voltages, this software also makes it possible to easily monitor individual cells for undervoltage and overvoltage and control the cell balancing function. Advanced users also have the option of writing entire program sequences with which they can verify a complete run of the monitoring and control of a Li-Ion battery. These sequences can also be executed in step mode to make simple debugging of such sequences possible.

With circuits such as the ATA6870 and the ATA6871, it will be possible to develop high-performance batteries in future that are cheaper, more efficient and more reliable than is currently possible. This is another step in support of the triumphant success of electrical and hybrid electrical vehicles.

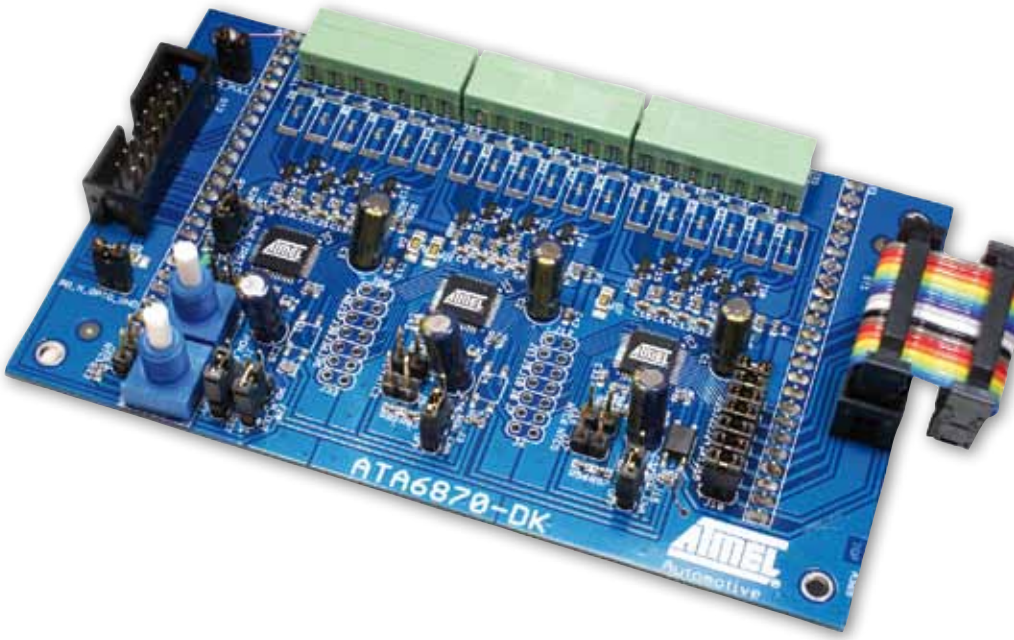

Security

Car Access

ATA5279 Multi-channel LF Antenna Driver

Gerd Edler

Introduction

Passive Entry (PE) and Passive Entry Go (PEG) systems are well-established in current luxury vehicles. The increasing demand for more convenience features, however, will pave their way also into medium-class cars. Consequently, cost-efficient electronic system solutions are required that use devices with high integration levels.

Atmel's intelligent 6-fold LF antenna driver ATA5279 manufactured using Atmel's own SMART-I.S.™ technology is a dedicated interface device targeting this application segment. Its main features as well as application and tool-related aspects will be covered in this article.

Principle of Passive Entry

A car key is powered by a small Lithium battery that supplies the internal microcontroller and the associated UHF transceiver with an LF wake-up signal. Most of the time, however, the key remains in sleep mode to minimize the current consumption and thus extend the battery lifetime.

A key wake-up is initialized by touching one of the vehicle's door handles, which causes the microcontroller to send a wake-up signal via the LF antenna that is located in the corresponding door handle (see figure 1). If the key's LF receiver has detected an appropriated LF wake-up signal, a UHF ID response is sent back to the microcontroller.

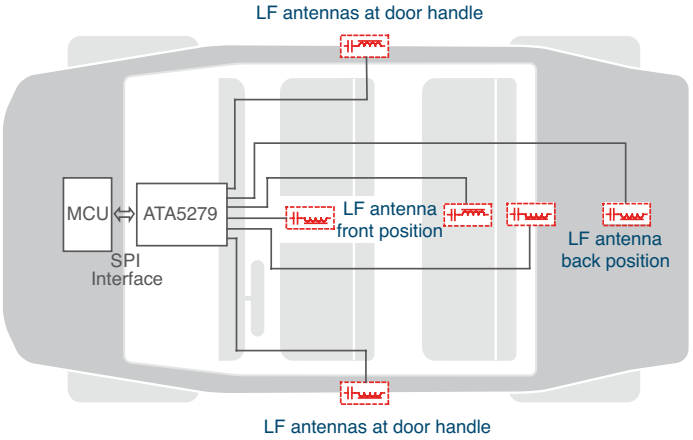

Figure 1. Typical LF Antenna Arrangement in a Vehicle

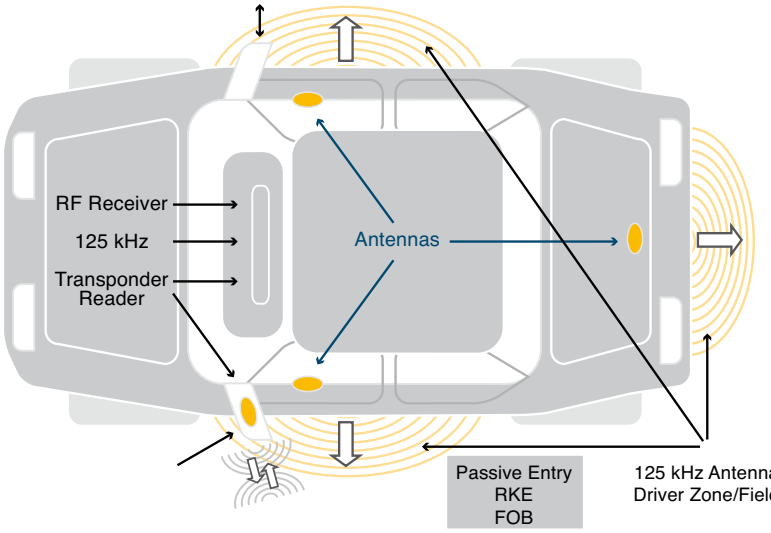

Figure 2. LF and UHF Communication Channels Typically Used for Vehicle PEG

After a mutual authentication processed by the UHF channel, the car door opens. 6 LF antennas are used to determine whether the key is located inside the vehicle; PE systems in luxury cars sometimes even use up to 9 antennas.

ATA5279 Multi-channel LF Antenna Driver

The ATA5279 is designed and qualified with regards to automotive PE/PEG systems and thus provides the features required for those applications:

- Six antenna driver stages provide a peak current of up to1000/700 mA
- Boost converter for stabilized antenna current is widely independent of battery voltage and antenna tolerances
- Sinusoidal 125-kHz antenna driving signal to minimize radiation of harmonics

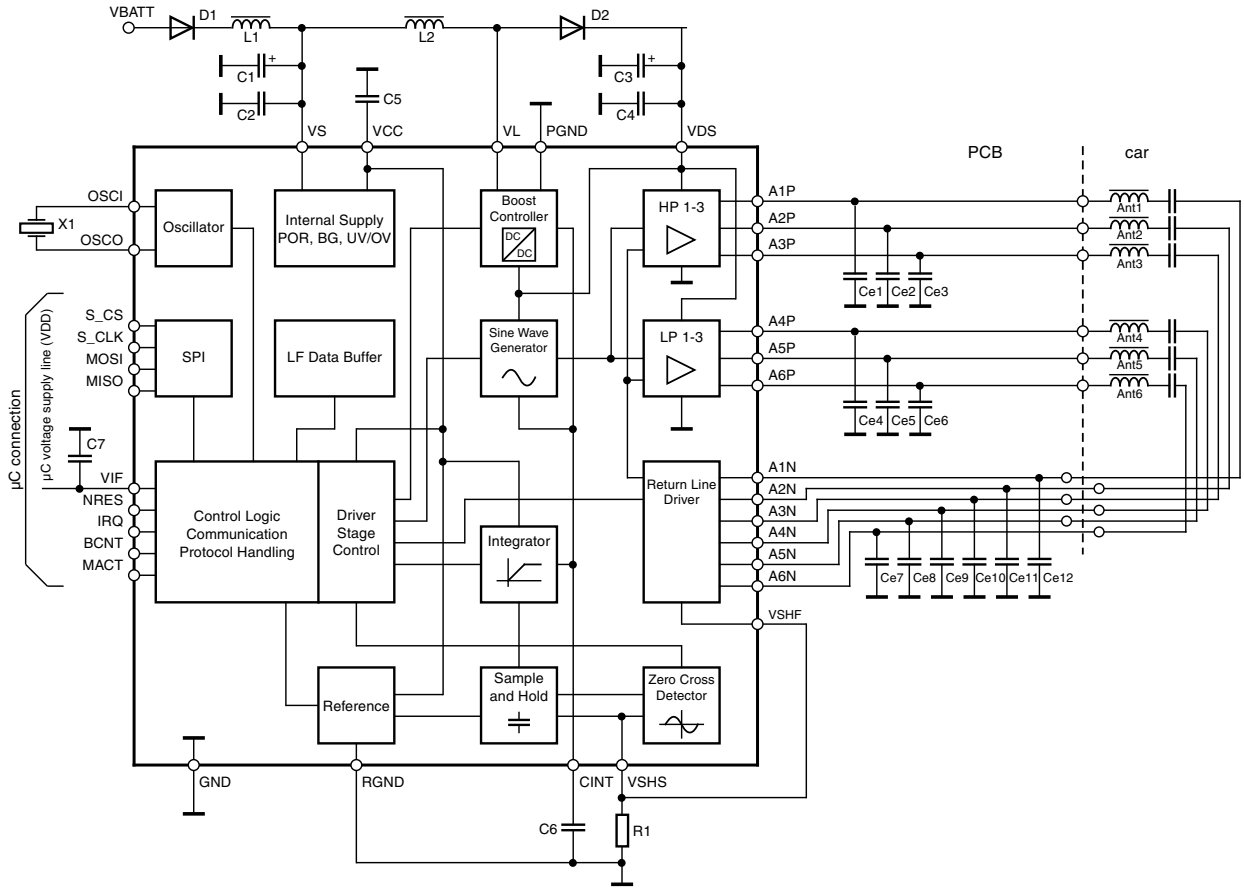

Figure 3. Typical Applicationa Using up to 6 LF Antennas

- Antenna current regulation is programmable by 20 set-point levels needed for RSSI field strength measurement
- LF data buffer to exonerate the MCU from data transmission task
- Advanced fault diagnostic for driver and antenna indication
- Fully protected against electrical and thermal overload
- SPI interface suited for bus structure designs, supports most members of Atmel's AVR microcontroller family
- Very low power-down current consumption
- Small 7 x 7 mm QFN48 package

Description of Main Features

Driver Configuration

The ATA5279 includes 6 push-pull driver outputs. AP1 to AP3 are specified with a peak current of typically up to $1A_P$, and AP4 to AP6 are designed for $0.7A_P$. The difference is due to the fact that PE near-field antennas can be driven with lower currents. Connected antennas are usually matched by a capacitor on the module to a resonant frequency of 125 kHz. The antenna return line driver is used to decouple the inactive antennas from current sensing to avoid parasitic impacts. The common supply voltage VDS of the driver stages is generated by the internal boost converter and is tracked by the current regulator according to the programmed set-point.

Boost Converter, Driver Signal and Antenna Aspects

Both, the boost converter voltage VDS supplying the driver stages as well the sinusoidal driver input signal, are controlled by the current regulation unit. Since the amplitude of the sine wave does not reach the VDS supply rail level (a delta of 3V remains), the dynamic range $V_{OUT,min}$ to $V_{OUT,max}$ is 34V maximum, related to V_{DSmax} = 40V (see figure 4). Thus the maximum antenna impedance can be calculated as follows.

$$\max|Z_{tot}| = \frac{V_{Out,\max} - V_{Out,\min}}{2 \cdot I_{Ant}}$$

For example, to drive a maximum antenna current of $0.7A_P$, the total impedance $\max|Z_{tot}|$ needs to be less than:

$$\max|Z_{tot}| = \frac{34V}{2 \cdot 0.7\ A_p} = 24.2\Omega$$

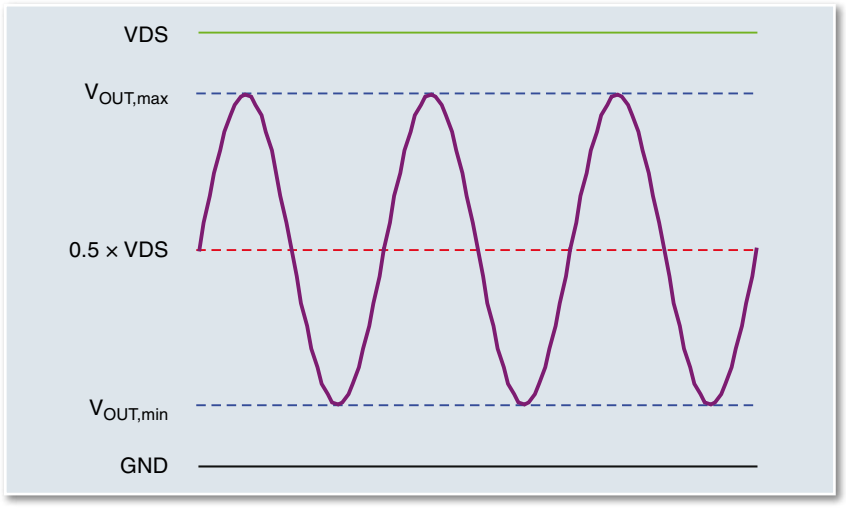

Figure 4. Sinusoidal Driver Signal Depending on VDS of the Boost Converter

The sole antenna impedance is reduced by the shunt resistance and by R_{DSon} of the return line switch.

$$|Z_{Ant}| = max|Z_{tot}| - R_{Shunt} - R_{Dson,RS}$$
$$= (24.2 - 1 - 1.2)\,\Omega = 23\Omega$$

However, antenna impedances lower than 10Ω should not be used because they might be indicated as erroneous.

Remark: Non-resonating antennas also need an additional capacitor to decouple the DC offset of the sine-wave driver signal.

The selection of the maximum antenna inductivity is geared to the chosen LF bit rate (BR) according to the following equation:

$$\max L_{Ant} = \frac{Q \cdot |Z_{Ant}|}{2 \cdot \pi \cdot f}$$

where

$$Q = \frac{f}{BR}$$

Minimization of Radiated Antenna Harmonics

Even though the power dissipation of the driver stage exceeds that of a driver with a square-wave output (such as with ATA5278, for example), a sinusoidal antenna driver signal helps to minimize the radiated harmonics and thus both effort and cost to meet the EMC approval. In terms of EMC, the reference measurements of the spectral analyses (see figures 5 and 6) illustrate the advantage of the ATA5279's sinusoidal driver signal. Both drivers were operated under the same conditions with an antenna current of 700 mA_P.

Antenna Current Regulation

The antenna current is regulated by the boost driver voltage VDS whose current is widely independent of the battery state and also of the antenna tolerances. To enable an accurate field strength measurement by the PEG LF receiver, the antenna current (field strength) can be programmed via SPI in 20 predefined current set-points from 50 mA to 1000 mA.

LF Data Buffer

To ensure that larger LF data protocols (>2 bytes) can be sent seamlessly without loading the microcontroller, a 128-bit data buffer, organized in16 bytes, is implemented. All driver-related commands and data are stored as well as processed by the FIFO buffer. During operation the status is continuously monitored. An interrupt to reload the buffer via SPI can be executed with up to 2 Mbit/s.

Protection and Diagnostic Features

In **operation mode** all driver connection lines AxP and return lines AxN are monitored. If one of these lines has a short to battery supply or to ground, or if an antenna is shorted, the power stages switch to shut-down mode to protect themselves from damage. In addition, the temperature sensors on the NMOS driver stages also shut down if temperature exceeds 140°C. Simultaneously to the shut down, an interrupt request is triggered and the shut-down cause is stored in the fault register.

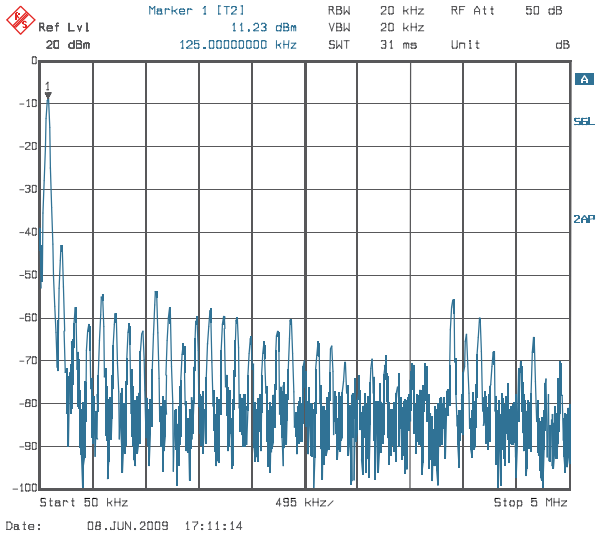

Figure 5. Spectral Analysis of ATA5279

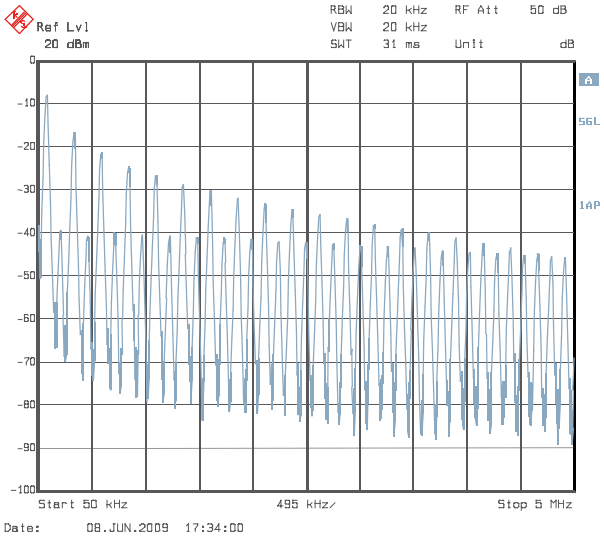

Figure 6. Spectral Analysis of ATA5278

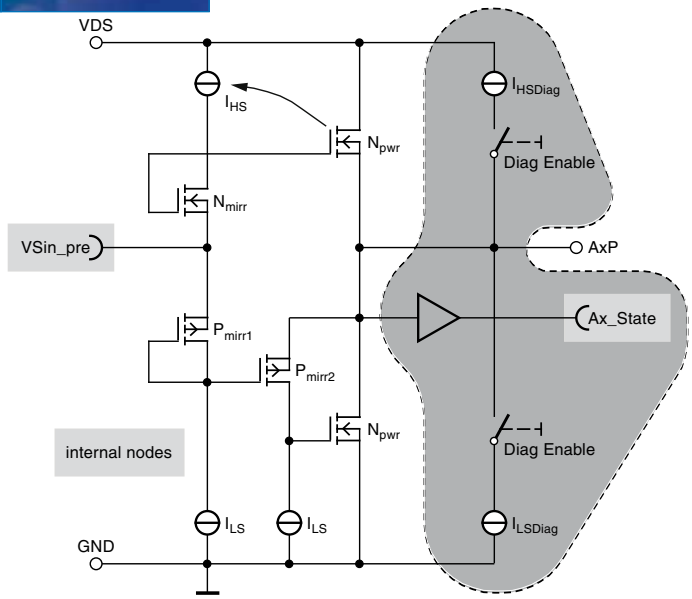

Figure 7. Principle of AxP Driver Arrangement

Further, an advanced **diagnostic mode** allows to load the AxP and AxN outputs by switchable DC current sources (see figure 7, gray area). During this mode the driver stages remain in high impedance. The diagnostic mode also enables to set the current switches, and the digital level state of the selected AxP and AxN stages can be read via a status request. This mode, alongside with the related test structures, can be used to indicate any antenna-line interconnection faults.

Application Tools

To support design-in of the ATA5279 driver IC, Atmel provides an evaluation kit with PC software (ATAB5279_82) at http://atmel.com/dyn/products/tools_card.asp?tool_id=4371. This kit can be ordered via Atmel's local distribution partners.

The kit features LF wake-up functionality using the 6-fold LF antenna driver ATA5279 in combination with the 3D LF receiver ATA5282. The ATA5279 driver capability combined with the included antenna module enables a receiver wake-up distance of up to 3 meters.

The ATAB5279 driver board (see figure 8) is patched onto the microcontroller baseboard ATAB-LFMB-79. The mounted AVR® microcontroller ATmega8515 is programmed in C-language and enables both to control the antenna driver and to maintain the communication with host. Operating software for host installation is provided on CD-ROM.

Application Using 9 Antennas

As explained earlier, certain luxury-car PEG applications require more than six LF antennas. Figure 9 illustrates a proposal how to expand the standard 6-fold antenna IC ATA5279 to also drive nine antennas. In this case A6P is the common driver of four antennas, whereas the antenna return lines are multiplexed by two dual NMOS transistor devices. A corresponding application note is available on request.

Figure 8. Evaluation Kit ATAB5279-82

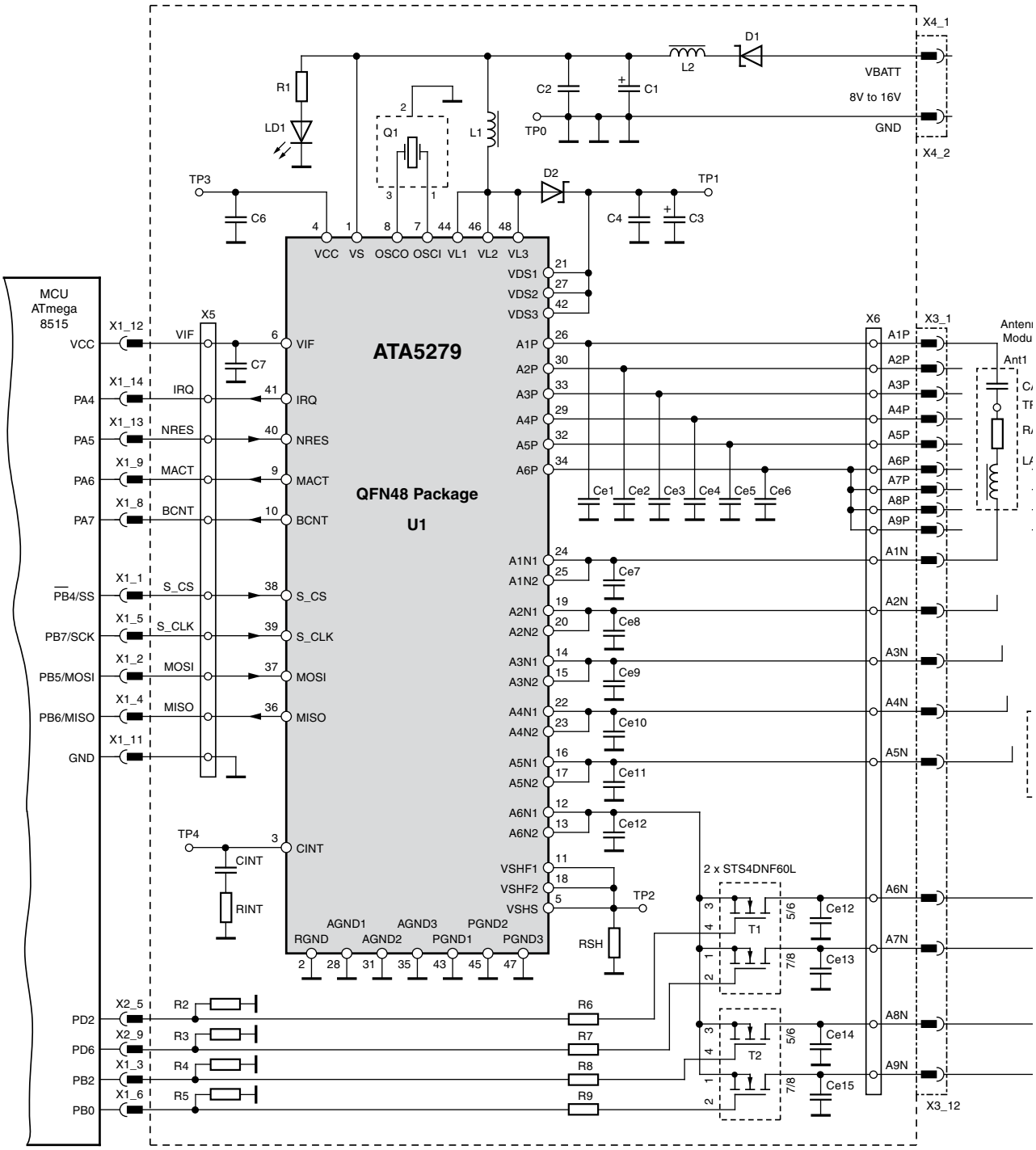

Figure 9. 9-antenna Application

Security

Car Access

RF Design Considerations for Passive Entry Systems

Paul Lepek, Paul Hartanto

Introduction

Passive Entry (PE) systems set a new trend for automotive comfort and security. Although they were available already years ago, they have become more popular recently as their increased integration level allows for lower system costs.

While Remote Keyless Entry (RKE) systems are fully interactive – the user must push the key to open the door – PE systems are passive, i.e., they do not require any interaction by the user to unlock the door. In a PE system, a low-frequency (LF) signal is transmitted, which is usually triggered by pulling the door handle when entering the vehicle. The key fob receives the LF signal within a few milliseconds, encrypts the received challenge data packets and returns the cipher payload via the RF channel back to the vehicle for authorization.

Passive Entry Systems can also include a passive engine start function, also called Passive Entry Go (PEG). Once the system has verified that key fob is inside the vehicle, the driver's presence in the seat triggers the LF field. When authentication has been granted and the position measurement has been made, the engine can be simply started by pushing a start button.

In both cases the plain text data is received by the key fob and encrypted by using a powerful encryption hardware module (e.g., AES-128 module). Cipher data is then returned to the vehicle for verification.

The PE key fob is powered by a small lithium battery which provides power for data reception, encryption and transmission. Key fobs used in passive entry systems are designed to ensure longest possible battery lifetime. If the battery runs low, a so called emergency mode couples enough magnetic fields via its LF coil to enable operation without battery. This requires positioning the key fob close to the door coils. In this case the communication occurs only via the LF channel.

A Typical PE System

A typical PE system consists of a vehicle and a key fob sub-system,

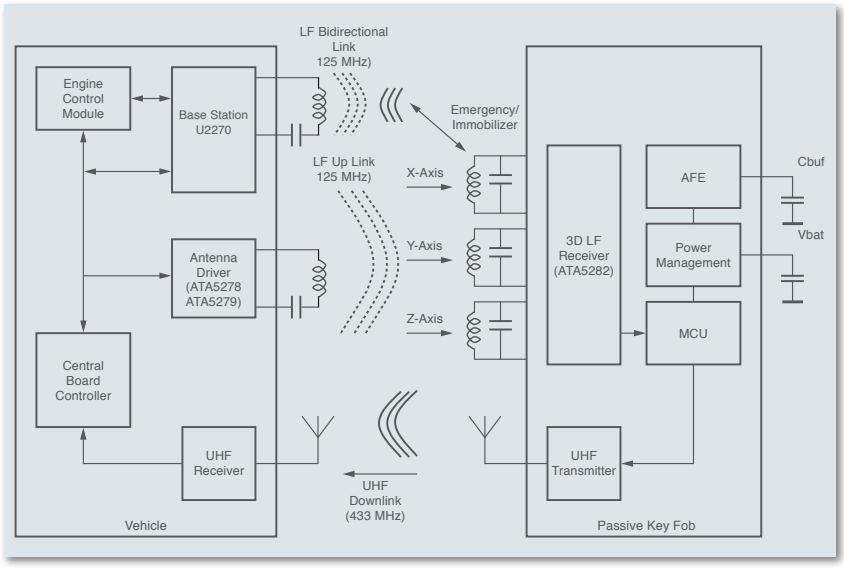

Figure 1. Passive Entry System Block Diagram

which serve as communication peers establishing two communication links: (1) LF uplink: vehicle-to-key fob, (2) UHF downlink: key fob-to-vehicle (see figure 1).

Vehicle

The LF field is generated by the antenna driver in the vehicle when a user pulls the vehicle door handle. The switch activates the request to the central board controller to initiate LF communication with the key fob. The antenna LF coils are usually placed in each car door, and are driven by the antenna driver unit (there may be more antenna coils driven by one antenna driver; e.g., the ATA5279 is able to drive up to six different antenna coils). To support the RF link, a UHF receiver module is used to receive RF data from the key fob. Received cipher data is then routed back to the board controller and decrypted by the software (AES[1]-128).

Key Fob

In any PE system, a key fob must be able to measure the LF signal strength on three orthogonal axis (X, Y and Z direction), and transmit this information via the RF channel, using the UHF transmitter, back to the vehicle to determine the key's position. This signal strength information – also known as Remote Signal Strength Indicator (RSSI) – is collected by using three orthogonal antenna coils connected to the 3D LF receiver. Any digital data, such as wake-up data pattern (preamble, ID), system commands or a plain text data challenge used as a payload in the protocol, is received and passed to the key fob MCU for processing (return message assembly, encryption). To save power, the LF receiver includes a dedicated control logic which can parse and check the wake-up signals with very low power consumption. A full system wake-up is not needed. This function can greatly extend a key fob's battery lifetime. A small 8-bit ultra low-power MCU (e.g., ATtiny44) can be used to control the data traffic into and out of the fob. Received data can be ciphered either via software or by a hardware crypto module with powerful encryption capabilities (e.g., AES-128). For increased security, a crypto mechanism is both implemented into the hardware and embedded on the MCU. Once encrypted, data is routed to the UHF transmitter where it is transmitted to the vehicle at a high baud rate.

In case a battery is completely discharged, the transponder can also operate as a passive device without battery. This is known as emergency mode. In this mode, only one of the orthogonal coils is used to couple to the LF magnetic field and to obtain sufficient energy as a charge on the Q-store external capacitor. The transponder communicates with the base station via the LF link to open the doors, and is used as an immobilizer to start the engine (see figure 1, where the X-axis coil acts as a 3D LF receiver coil and an emergency/immobilizer

PE System Feature	Characteristics
Position measurement	- LF field measurement on three orthogonal axis (X, Y, Z) - Range up to 3 m - High receiver sensitivity required for RSSI measurement, data reception
Data communication	- LF unidirectional only (125 kHz, uplink, up to 3.9 kbaud) - RF (315, 433, 868, 915 MHz) uni/or bidirectional, downlink/uplink (up to 20 kbaud) - LF bidirectional (125 kHz, up to 3.9 kbaud) – emergency mode/immobilizer application without battery
Battery and battery-less operation	- Extended lifetime due to use of small Lithium-cell battery as a Passive Entry key fob - Emergency door unlock function (low battery condition) - Immobilizer function via one LF antenna coil
Data security	- Crypto module in hardware (AES-128) - Secure crypto key storage - Secure communication protocol

Table 1. Fundamental PE System Parameters for a Key Fob

[1] *Advanced Encryption Standard is an encryption algorithm approved by National Institute of Standards and Technology. AES was originally published as Rijndael algorithm. NIST is a measurements standards laboratory which is a non-regulatory agency of the United States Department of Commerce.*

transceiver antenna). The Analog Front End (AFE) module is used for LF communication, while the Power Management (PM) module manages field supply power as charge stored on the external storage capacitor, C_{buf}. RSSI measurement, 3D LF data reception and RF transmission are disabled in emergency mode.

Receiving LF Signals

The LF field with its carrier frequency of approximately 125 kHz can be used as: (1) a data communication link transmitting data at low baud rates, (2) a medium to compute positioning information-RSSI values on three axes, (3) an electromagnetic contactless medium to transmit electrical energy over short distances. Each of those application types and its transmission quality, however, relies on the transmitter-to-receiver antenna coupling. Coupling depends on many physical and electrical parameters such as antenna inductance, resistance, coil-to-coil distance, resonance tuning, etc. The greater the coupling factor the stronger the communication link (i.e., improved energy transfer from coil to coil).

An LF electromagnetic signal radiated from a transmitter coil antenna propagates with a certain directional angle at which the magnetic field is strongest, and decays as moved away from its center. To achieve optimum antenna coupling, the transmitter antenna must directly face the receiver antenna. By using orthogonal receiver antennas placed on X, Y and Z axis, the directionality of single transmitter antenna is circumvented. In return, multiple receiver antennas placed at 90 degrees from each other enable signal reception from any given direction by a different antenna coil.

RF Communication in Passive Entry Systems

Atmel offers a broad range of UHF ICs designed for uni- or bidirectional communication in the ISM frequency range, thus serving automotive applications such as car access systems. This comprises the T5750/53/54, ATA5756/57 transmitter family, and the ATA5723/24/28, ATA5745/46

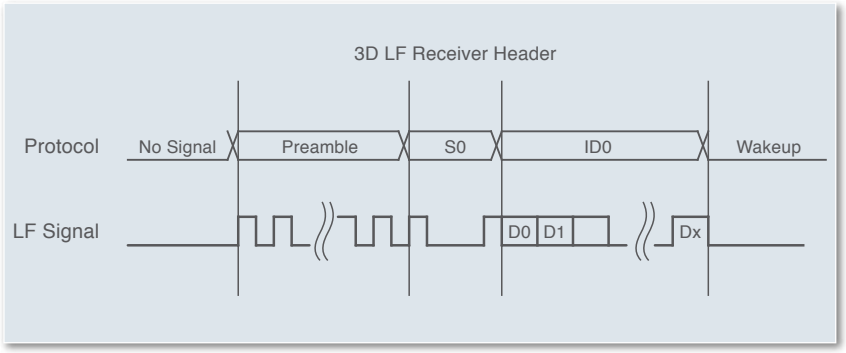

Figure 2. 3D LF Receiver Wake-up

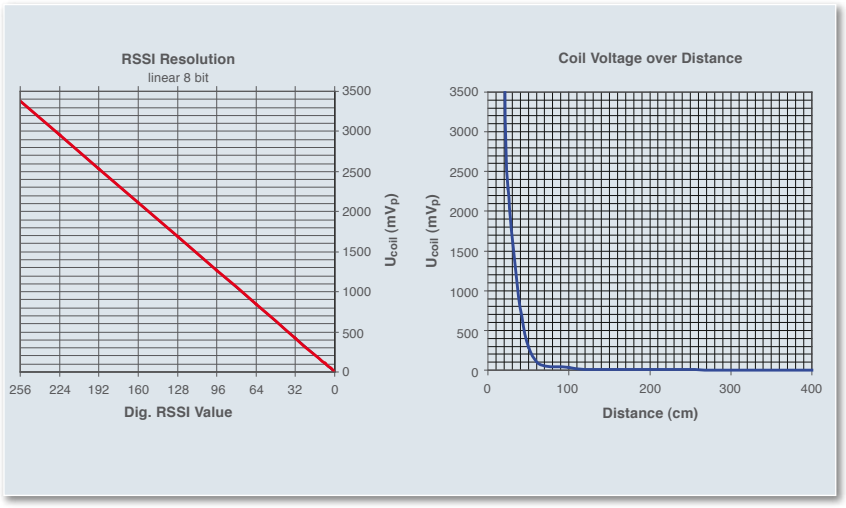

Figure 3. Position Measurement – RSSI

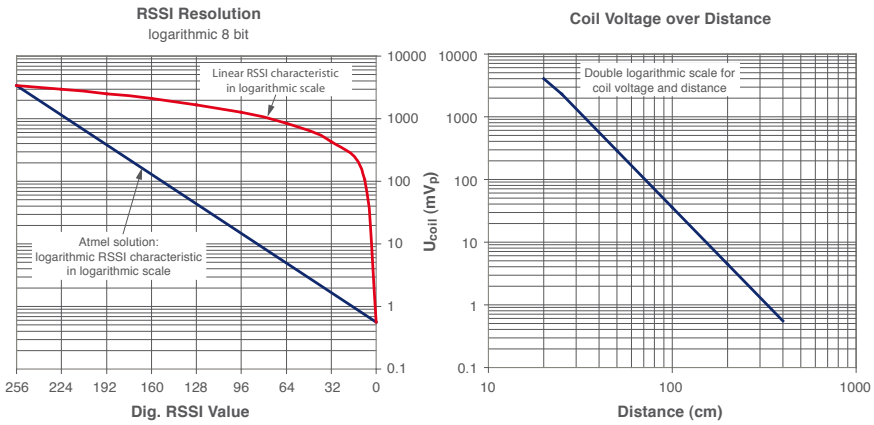

Figure 4. RSSI Resolution

receiver family for unidirectional communication. For bidirectional communication, the transceiver families ATA5811/12 and ATA5823/24 are available. This chapter discusses some general RF considerations which must be taken into account when designing a passive entry system.

The most discussed RF design issues are the achievable distance and, of course, the system reliability. In general, an RF system consists of a transmit module – in this case a key fob – and a receive module. The transmit power and the sensitivity are the main parameters that need to be considered well in order to design the best solution. Atmel's transceiver IC ATA5824, for example, provides an excellent FSK sensitivity of -109 dBm typ. (at a data rate of 2.4 kBps) and a transmit power of 10 dBm typ., which helps to achieve an outstanding distance for a car access system.

Antenna Performance

In addition to RF parameters such as transmit power, sensitivity, etc., the antenna performance is important to obtain an optimal system link budget and thus the largest distance possible. In most cases, the antenna design is a compromise between the available space and the antenna size. Due to this, it occurs quite often that the optimum antenna geometry can not be implemented in the key fob, where a small loop antenna is preferred. A loop antenna is a magnetic antenna. In key fob applications, this antenna type is more beneficial than a whip antenna, because the loop antenna is less sensitive regarding contact with the human body. Some applications may require a highly efficient antenna due to the long transmission distance, so a (folded) whip antenna might be the appropriate key fob solution. Some antenna manufacturers offer chip antennas whose Q factor and gain are relatively high, compared to printed antennas. This could also be a good solution if the system costs are not a crucial factor. In the vehicle, the antenna size is not critical. Some cars use antennas implemented in the window (e.g., rear window), but the most popular solution is the printed antenna which is located on the receiving module's PCB. Table 2 summarizes the advantages and disadvantages of these two antenna types.

Both the behavior of the vehicle antenna as well as that of the key fob antenna is not isotropic. Figure 5 illustrates the 2D radiation pattern of both antennas. Due to this, the maximum and minimum values must be defined at the beginning of a design. This is not a simple issue, of course, but a maximum and minimum allowed attenuation due to the radiation pattern can be used as a starting point.

Ground Bounce Reflection

In real life, the environment influences the attenuation of the system link budget due to reflection and fading effects, which must be taken into account when defining the system's link budget. The following calculation example shows

Antenna Type	Advantage	Disadvantage
Integrated antenna on window	Better antenna performance since the antenna is outside of the car body	The assembly and antenna manufacturing costs are much higher
Printed antenna on board	This solution is much cheaper	As both the module and the antenna are within the car, the antenna performance will not be optimum

Table 2. Advantages and Disadvantages of Different Antenna Types

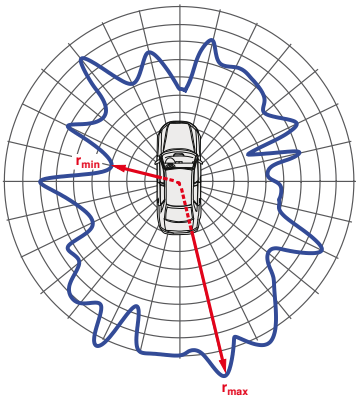

Figure 5. Example of a Possible Antenna 2D Radiation Pattern of a Vehicle

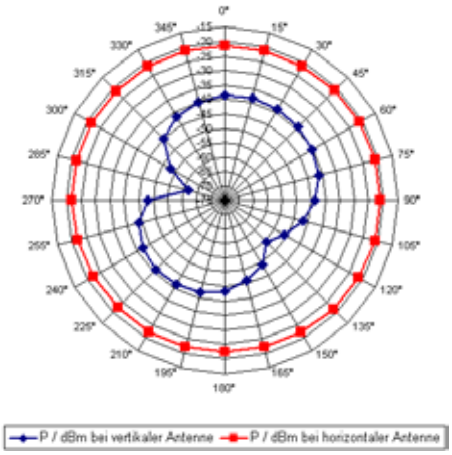

Figure 6. Example of a Possible Antenna 2D Radiation Pattern of a Key Fob

the influence of the ground bounce reflection on the achievable distance:

Example

- Receiver sensitivity: -109 dBm typ. at 433.92 MHz
- Transmit power: is 10 dBm typ.
- Transmitter antenna gain: -18 dB (which is close to the small loop antenna performance)
- The receiver's antenna gain is assumed -6dB in this case

If the ground bounce reflection can be disregarded, a distance of approximately 3 km can be calculated, based on the free-space equation. In case the ground bounce reflection is taken into account, the typical achievable distance reduces to about 300 m. In reality, the ground bounce effect is much more complex than in this example, of course. Figure 7 illustrates how the reflection effect influences the power received at the vehicle antenna. The red curve shows the ideal behavior under free-space conditions, whereas the blue curve shows the behavior if somebody is walking slowly towards the car.

Blocking Performance

An RF system is always subject to environmental interferences; especially within a car, there is a lot of noise and disturbances. To provide the best solution for such applications, Atmel's car access devices feature excellent blocking performance. As an example, figure 8 shows the 3-dB blocking curve of ATA5824 at 433.92 MHz. In some cases, however, the blocking requirements are substantially higher than the integrated circuit is able to fulfill. To meet such extended application needs, an external front-end SAW filter helps to improve the blocking performance.

IF Filter Bandwidth

Another important criterion for the system definition is the intermediate frequency (IF) filter bandwidth. All system frequency tolerances must be considered well with respect to this parameter. The crystal tolerance as well as the crystal oscillators for both receiver and transmitter must be specified well so that even in worst case the transmitter spectrum will still be received

Figure 7. Effect of the Reflection on the Received Signal Power at 868 MHz System

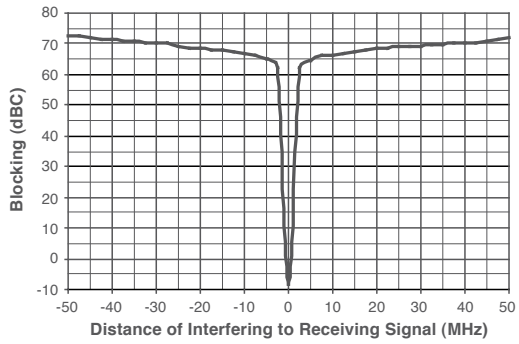

Figure 8. Wideband 3-dB Blocking Characteristic of ATA5824 at 433.92 MHz

within the IF filter bandwidth. For a system with extremely narrow IF bandwidth, the data rate as well as the modulation type (excluding the tolerances) must also be taken into account.

Current Consumption

The current consumption is always a main issue in car access systems, especially in the key fob module. Today's required battery lifetime is approximately 7 years. Even though the current consumption requirements on the vehicle side do not seem to be that high, a low power solution is mandatory as the number of electronic modules within a car increases constantly. Atmel's UHF devices are specifically designed to meet such low power requirements.

Current consumption examples of selected Atmel ICs:

- Transparent receiver IC ATA5745: 6.5 mA (typ.) in active mode
- Receiver IC ATA5724: 8 mA (typ.) in active mode
- Transmitter IC T5754: 9 mA (typ.) for 7.5 dBm power
- Transceiver IC ATA5824: 10.5 mA (typ.) both in receive and transmit mode (P = 5 dBm)

Some methods can also be applied to further reduce the average current consumption. The transmission of a higher data rate for a defined telegram length is one example. Less current is consumed due to the shorter transmission duration. The On/Off Keying (OOK) modulation can be beneficial over Frequency Shift Keying (FSK) when it comes to lowering the average current consumption of a transmitter. The best way to reduce a receiver's current consumption is to switch it between sleep and active mode so that the entire circuit remains active as if a valid signal is coming. For this purpose, most Atmel receiver and transceiver ICs feature polling mode.

References

1. Atmel Datasheet "Stand-alone Antenna Driver IC ATA5278", see http://www.atmel.com/dyn/products/product_card.asp?part_id=3520
2. Atmel Datasheet "Read/Write Base Station IC U2270B", see http://www.atmel.com/dyn/products/product_card.asp?part_id=2380
3. Atmel Application Note "Electronic Immobilizers for the Automotive Industry", see http://www.atmel.com/dyn/resources/prod_documents/doc4661.pdf
4. Atmel Application Note "AVR411: Secure Rolling Code Algorithm for Wireless Link", see http://www.atmel.com/dyn/resources/prod_documents/doc2600.pdf
5. Atmel Datasheet "UHF ASK/FSK Transceiver IC", ATA5823/ATA5824, see http://www.atmel.com/dyn/products/product_card.asp?part_id=3778 (ATA5823), http://www.atmel.com/dyn/products/product_card.asp?part_id=3779 (ATA5824)
6. Atmel Datasheet "UHF ASK/FSK Transmitter IC T5753", see http://www.atmel.com/dyn/products/product_card.asp?part_id=4128
7. Atmel Datasheet "UHF ASK/FSK Transmitter IC T5754", see http://www.atmel.com/dyn/products/product_card.asp?part_id=4129
8. Atmel Datasheet "UHF ASK/FSK Receiver IC", ATA5743/ATA5744/ATA5745, see http://www.atmel.com/dyn/products/product_card.asp?part_id=3647 (ATA5743), http://www.atmel.com/dyn/products/product_card.asp?part_id=2864 (ATA5744), http://www.atmel.com/dyn/products/product_card.asp?part_id=3961 (ATA5745)
9. Atmel Datasheet "UHF ASK/FSK Receiver IC" ATA5723/24/28, see http://www.atmel.com/dyn/products/product_card.asp?part_id=4216 (ATA5723), http://www.atmel.com/dyn/products/product_card.asp?part_id=4217 (ATA5724), http://www.atmel.com/dyn/products/product_card.asp?part_id=4218 (ATA5728)
10. Federal Information Processing Standards Publication 197, Announcing the Advanced Encryption Standard (AES), Nov. 26, 2001. AES page available at http://www.nist.gov/CryptoToolkit.4
11. J. Daemen and V. Rijmen, AES Proposal: Rijndael, AES Algorithm Submission, September 3, 1999.
12. Paul Kocher, Design and Validation Strategies for Obtaining Analysis and Related Attacks, http://www.cryptography.com

Security

Car Access

Predicting RF Range Performance

Ahmad Chaudhry, Jim Goings

Overview

For the automotive engineer using a radio to communicate across some distance, range capability is inevitably a primary concern. Whether it's someone trying to unlock a car door, a consumer trying to remotely start a car, or a driver opening a garage door from the car, an expectation for reliable communication always exists.

On what do the quality, robustness, and range of any RF communication link primarily depend? Simple – the physics of electro-magnetic wave behavior.

The equation defined by H.T. Friis which describes this wave behavior in free space, called the Friis Transmission Equation, is:

$$P_R = P_T G_T G_R \left(\frac{\lambda}{4\pi}\right)^2 \left(\frac{1}{d}\right)^n$$

(Equation 1)

where

P_R = power received (watts)
P_T = power transmitted (watts)
G_T = gain of transmit antenna (scalar)
G_R = gain of receive antenna (scalar)
λ = wavelength (metric or English)
d = distance separating transmitter and receiver (metric or English)
n = exponent for environmental conditions (n = 2 defines "free space")

Essentially, this equation states that the strength of the electro-magnetic radio wave received at some location is a function of: (a) the strength of the original transmitted signal, (b) the performance of the antennas at the transmitter and receiver, (c) the wavelength corresponding to the frequency of operation, and (d) the distance separating the transmitter and receiver.

In technical literature, this equation is sometimes expressed in other forms. It might be solved for a different variable; or, re-arranged into a "Path Loss" equation; or, written with additional terms, to give more detail; or, simply re-written in "dB" (decibel)* units, a logarithmic measure. In yet another form, the Friis Equation is used for a common communication system performance analysis called a "link budget". A sample of some of these alternative forms is shown in the appendix of this article. It's worth emphasizing that equation 1 considers only the electromagnetic characteristics of the RF field, nothing more. "Smart" data transmission and received-signal processing techniques can compensate for marginal field strength levels in order to achieve an otherwise less-than-reliable communication link. However, this is beyond the scope of this article.

RF in a Real-world Environment

Modeling or predicting radio wave behavior in a real-world environment is an exercise always characterized by uncertainty. Using Friis' Equation with free-space conditions is a good "first approximation" but it can be, as can be seen in this section, quite inaccurate. The effects of "multi-path" wave propagation, separation distance, low transmitter output, poor receive sensitivity, and inefficient antennas all contribute to reduced communication range. Let's look at these influences with a level of detail appropriate for each.

Multi-path Wave Propagation

First, consider the phenomenon of wave travel known as "multi-path". When a wave leaves the antenna, it

travels in all directions. “Multi-path” describes the situation in which the wave is modified by its propagation through the environment, before arriving at the receiver. These waves incident on the receiver’s antenna are categorized into four types:

(1) **direct waves:** ones which travel on a line-of-sight path
(2) **reflected waves:** ones which bounce off smooth surfaces that are much greater than one wavelength in size for the specific operating frequency
(3) **diffracted waves:** ones which are bent around sharp corners
(4) **scattered waves:** ones which bounce off objects or features on a rough surface that are much smaller than a wavelength in size

Waves which are diffracted, reflected, or scattered experience changes in magnitude and phase, additional to what naturally occurs to a direct wave. These variations in magnitude and phase are caused by (1) absorption of some of the wave’s energy by the reflecting surface, (2) the phase change caused by a reflection, and (3) the differences in length of the paths traveled by the various waves. These multi-path waves arrive from many angles and directions, causing them to sum with various magnitudes and phases at the receiver. As a result, the composite wave at the receiver can be either greater than or less than what would be produced by the direct wave alone. This means that some waves add to the direct signal and some subtract from it. The worst case could total cancellation, yielding no detectible signal at all. Thus, it can be quite difficult to predict a transmitted wave’s behavior because of the multiple paths it takes before arriving at the receiver.

Loss as a Function of Distance (the “n” Exponent)

Next, it is considered how the separation distance between the transmitter and the receiver affects the signal strength at the receiver. Since radio waves behave much like sound waves, a parallel can be drawn here. As one is distanced further and further from a sound’s source, the sound one hears is weaker. The same is true for radio waves. In the Friis Equation, the factor which affects the strength of a radio wave received at some distance from the transmitter is:

$$\left(\frac{1}{d}\right)^n$$

(Equation 2)

where “d” is the separation distance between the transmitter and receiver. Friis determined that n = 2 accurately characterizes wave behavior in an environment absent of anything which alters the wave’s travel. In equation 1, this was defined as the free-space environment. When n = 2, this means that the strength of the received radio wave is proportional to the square of the distance separating the transmit source and the receiver. To make sense of this, here are some easy-to-remember guidelines which help make quick range estimates using the free-space case.

Doubling the distance separating the transmitter and receiver reduces the received signal strength by:

- 1/4th as a fractional scalar, or
- to 25% of the original value, as a percentage, or
- 6 dB as a decibel value

On a larger scale, increasing the separation distance by a factor of 10 reduces the received signal strength by:

- 1/100 as a fractional scalar, or
- to 1% of the original value, as a percentage, or
- 20 dB as a decibel value

The real world, however, is not an ideal free-space environment. RF waves are altered (bent, diffracted, reflected, attenuated, absorbed, etc) as they propagate. Because of this, Friis' free-space equation gives at best an approximation. Assuming a free-space environment as a baseline does, however, provide a couple of advantages when comparing multiple scenarios: (1) the environment is always consistent for a mathematical analysis, and (2) the resulting calculations are still an acceptable approximation. For critical, detailed, and more accurate evaluation, however, it is important to have a better model of the intended application environment. This leads to "n" values which are other than "2". Now let's consider some empirically-determined values for "n" for several types of environments.

The reason why the impact of the value of "n" on range is significant is because it is an exponent and not simply a multiplier. Several sources have published values for "n" which were determined by field measurements. Table 1 gives some of these values. Notice that they are rarely < 2, making the impact of separation distance even more significant in real-world situations. Nonetheless, with them the Friis Equation more realistically predicts wave behavior for real environments.

Environment	"n" Value
Free space	2
Grocery store	1.8
Retail store	2.2
Office (hard walls)	3
Office (soft walls)	2.6
Remote keyless entry	4

Table 1. Values for "n"

In addition to loss as a function of distance, other factors such as attenuation from obstacles and antenna loss affect overall RF performance. For more info on these topics please refer to the conclusion of this paper. [1]

Summing the Losses

An RF wave can experience significant degradation as it travels through a real-world environment, and these influences must be accounted for during the design phase if a communication system has any chance to perform to realistic expectations.

So, when considering reduced receiver sensitivity, low antenna gains, distance between the transmitter and receiver, wave penetration through walls, and "n", how do all these factors combine mathematically to affect the range of a transmitted signal?

The best answer is found in exploring the next topic, "link budgets", where a modified form of the Friis Transmission Equation is discussed.

Link Budgets

The term link budget has already been introduced earlier. A link budget is simply an equation describing the performance of a communication link, accounting for all gains and losses in the RF-path elements of the link. A typical link budget equation looks like this:

$$P_R = P_T + G_T + G_R - (L_P + L_T + L_R + L_M)$$

(Equation 3)

where

P_R = received power (dBm)
P_T = transmitter output power (dBm)
G_T = transmit-antenna gain (dBi)
L_T = transmit-chain losses (coax, connectors, matching …) (dB)
L_P = path loss (dB)
L_M = misc losses (fading margin, body loss, polarization mismatch …) (dB)
G_R = receiver antenna gain (dB)
L_R = receive-chain losses (coax, connectors, matching …) (dB)

The elements in this link budget equation are essentially those of the Friis Equation, simply expressed with a bit more detail. Referring to

equation 5 in the appendix, equation 5, just like equation 3 above, is expressed in decibels (dB). When a "scalar" equation, such as equation 1, is converted to a logarithmic format such as these, multiplication and division is replaced by simple addition and subtraction.

Referring to equation 3, above, the "L" terms (L_P, L_T, L_R, and L_M) might appear to be new on first glance. Actually, though, three of them are in equation 1. The L_T and L_R terms are components of "P" and "G", respectively, and L_P represents the two components of path loss (see also equation 6). Only is L_M arguably a new term. It accounts for losses that one might unknowingly fail to factor into the calculation. By studying closely this link budget equation, someone unfamiliar with the total make-up of an RF communication link can quickly learn which of the various factors are involved and how they interact to affect an RF communication system's performance.

Link budget analysis is essential for designing a robust RF link. In preliminary assessment of the potential performance capability of an RF communication link, the requirements on each of the equation's elements can be determined. This is easily done by first identifying the terms in the budget equation which have "fixed" values in the real system, then substituting estimates for the remaining terms. Iterative substitutions of estimates will identify what constraints might exist on some of the other terms, or, at minimum, reveal realistic ranges for them. Later, the budget equation can be used with actual field-measured data to verify the performance of the link against these calculated expectations.

When using the link budget equation to predict system performance, it needs to be taken into account that the signal at the receiver P_R must be some minimum value, as determined by the receiver's sensitivity specification. Below that particular P_R value, the signal would be somewhere between marginal and unintelligible.

In equation 3, the L_M term is a very important component. This term is the "fading margin", and "margin" is the key word. Fading is essentially a time variation of the exponent "n" of equation 2, creating fluctuations in the signal levels at the receiver. These fluctuations are caused by changes in the environment in which the communication system operates. In order to have a robust communication system, it is imperative that sufficient margin for these fades be factored into the link budget equation. Otherwise during one such fade, communication may be disrupted or totally lost because of a marginal or unintelligible signal.

A recommended minimum fading margin (L_M) is 15 dB. This value, when added to the receiver's sensitivity specification, determines the minimum received signal level (P_R) that should be present at the receiver's front end. For example, a receiver with sensitivity of -107 dBm should have a minimum signal level (P_R) present at its front end of -107 dBm + 15 dB = -92 dBm.

The system design engineer has control over most, or potentially all, of the elements of the link budget equation. Constraints come from many sources, and they vary from application to application. Achieving maximum system performance from certain of these link elements can be simple, easy, and inexpensive alternatives. With other elements, it can be challenging. It is important, therefore, to carefully identify those elements over which one has control and plan for link-performance optimization accordingly.

A Range-calculator Spreadsheet

Table 2 shows a snap-shot of a range-calculator spreadsheet which was developed to provide

quick parametric analysis using the Friis Transmission Equation. The form of the Friis Equation used in the spreadsheet is shown. In the appendix, equation 8 is that same equation solved for the range, or distance, "d". The spread-sheet has six **input** parameters (orange text): transmitter output power, transmit-antenna gain, receiver sensitivity, receive-antenna gain, frequency of operation, and the "n" factor. The **output** (black text) is the calculated estimate of the communication link range.

TX output (dBm)	TX antenna gain (dB)	RX antenna gain (dB)
13	-15	3
RX sensitivity (dBm)	**Frequency (MHz)**	**Range (m)**
-120	315	656

"n" factor 3.5

Table 2. Range Calculator

governing equation, solved for "d":

$$P_{rcvd}\,(dB) = 20\,log\left[\frac{\lambda}{4\pi}\right] + 10n\,log\left[\frac{1}{d}\right] + P_{txd} + G_{TXant} + G_{RXant}$$

where

= required inputs

λ = wavelength (m)

π = 3.14159

P_{rcvd} = received power, or required receiver sensitivity (dBm)

P_{txd} = transmitted power

G_{TXant} = gain of the transmit antenna (dB)

G_{RXant} = gain of the receive antenna (dB)

n = range factor (2 – 4 typically)

Special Case: Remote Keyless Entry (RKE)

One of the most common applications utilizing a low-power UHF RF link is the automotive Remote Keyless Entry (RKE) system. Because some aspects of the environment in which RKE systems exists are predictable, special assumptions and geometric approximations can be applied to the Friis Transmission Equation when estimating communication range. These simplifications center around the fact that the RF energy arriving at the automobile has a multi-path reflection from ground which significantly affect the received signal received. This geometry is shown in figure 1.

The result of these simplifications to the Friis Equation is shown in equation 4. It calculates the signal loss in the path between the hand-held transmitter and the auto-mounted receiver. Note that the exponent, "4", for the distance variable, "d", is consistent with what was presented earlier in table 1 for the special case of RKE:

$$L_{PATH}\,(dB) = \frac{1}{2d^4}\left(\frac{h_{keyfob}^2}{h_{carRX}^2}\right)$$

(Equation 4)

where

h_{keyfob} = height of key fob above ground

h_{carRX} = height of in-car RKE receiver above ground

d = straight-line distance between key fob and car receiver

In deriving equation 4, these assumptions applied: (1) the wave phase shifts 180° when reflected by the ground, (2) the distance "d" is much greater than the height "h",

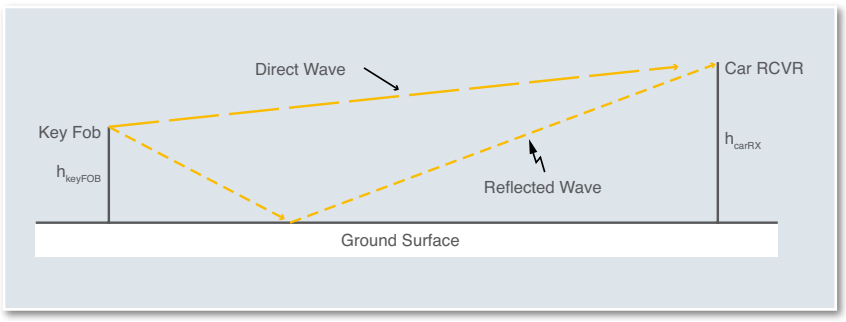

Figure 1. RKE RF-link Geometry

(3) the reflected-path distance is greater than the straight-line distance, and (4) half the transmitted power goes into the straight-line wave and half into the reflected wave.

The phase difference between the two waves (direct and ground-reflected) arriving at the receiver is frequency dependent. Between 300 and 400 MHz, this phase difference is somewhere around 90° when the key fob is within about 30 ft from the car. As a result, neither cancellation nor addition of the arriving waves occurs. In this situation, the free-space Friis Equation with n = 2 is a good approximation. It needs to be noted, however, that this is not a consistent predictor because a measure of phase variability exists in the ground-bounced signal. Even with the best approximations, the answer still is only a good approximation. When the key fob is further than 30ft from the car, a somewhat conservative “n = 4” is more accurate.

Consistent with the reason for developing the previous range-calculator spreadsheet, table 3 is a snap-shot of another one, specifically satisfying equation 4 for RKE systems.

P_{TX} (dBm)	G_{TX} (dB)	L_P (dB)	G_{RX} (dB)
13	-15	-121	3
P_{RX} (dBm)	Fade Margin (dB)	Range (m)	
-120	15	376	

Table 3. RKE Range Calculator

Inputs

P_{TX}: effective radiated power of transmitter

P_{RX}: sensitivity of receiver (or received power)

G_{TX}: antenna gain of transmitter

P_{RX}: antenna gain of receiver

Fade Margin: the additional signal strength desired so that, when fading

Calculated

L_P: path loss approximation

Range:

$$\left[10^{\frac{(P_L + 3 + Fading)}{40}}\right]^{-1}$$

It’s interesting to take note of how the simplifications in the RKE spreadsheet above using equation 4 gives rise to different results for the same scenario when calculated with the other spreadsheet (table 2). This further underscores the challenge the engineer faces when trying to predict range. While theoretical analysis is a noble effort, the fact that the environment in which we live is non-deterministic means that the obtained results will be, at best, an estimate of actual performance range.

Conclusion

For a more thorough look into range calculation, an expanded application note is available on the Atmel website (http://www.atmel.com/dyn/resources/prod_documents/doc9144.pdf). This document provides further explanation of terms in the Friis Equation, an expanded look into RF loss in the real world, and methods to improve RF range. In addition, two spreadsheets are available to manipulate system parameters while evaluating their effects on range.

Appendix

Formulas related to the basic Friis Transmission Equation.

Friis Equation in decibel form:

$$P_R\,(dB) = -20\,log\left(\frac{4\pi}{\lambda}\right) - 10n\,log\,(d) + G_T + G_R + P_T$$

(Equation 5)

Path loss in scalar form (where $G_T = G_R = 1$) :

$$L_{PATH} = \frac{P_R}{P_T} = \left[\frac{\lambda}{4\pi}\right]^2 \left[\frac{1}{d}\right]^n$$

(Equation 6)

Path loss in decibel form (where $G_T = G_R = 1$) :

$$L_{PATH}\,(dB) = P_R - P_T = 20\log\left(\frac{\lambda}{4\pi}\right) + 10n\,\log\left(\frac{1}{d}\right)$$

(Equation 7)

The generic Range Calculator spread-sheet equation solved for distance “d”:

$$d = 10\left[\frac{P_T - P_R - 20\,log\left(\frac{4\pi}{\lambda}\right) + G_T + G_R}{10n}\right]$$

(Equation 8)

Standard Products

BLDC Motor Control for High-temperature Applications

Rainer Boehringer, Matthias Piepke

Introduction

Even model-building enthusiasts expound the virtues of cars with so-called brushless motors without being explicitly conscious of it, since model cars with this technology are simply better.

In the automotive area, brushless motors are becoming increasingly important, since the advantages are obvious. Lighter BLDC motors are more efficient, and therefore reduce the energy consumption of the vehicle. At the same time, the simpler mechanical design and the eradication of brush wear increase the reliability and robustness of the motors, which is a key factor as far as customer satisfaction, is concerned. Electronic commutation reduces interference emission, and EMC requirements become easier to comply with. BLDC motor systems are therefore becoming increasingly important in many more automotive applications.

BLDC Motor Control Applications

BLDC motors are already used in fuel pumps, steering systems (Electronic Power Steering, EPS) and fan controllers for air conditioning systems. The quietness of these motors allows them to be used in convenience applications in vehicle interiors, such as power windows and air conditioning flap controllers.

Brush motors are only suitable for safety-related systems to a limited extent, since failure is predestined because of brush wear. However, when brushless motors are used, systems such as the ones used to cool Lithium-Ion batteries are more fail-safe.

The combination of electronic and mechanical systems leads to integrated motor control, and the system becomes even smaller. A sophisticated packaging and high-temperature technologies make it possible to use the motors in the immediate vicinity of the engine, allowing the system to be used in under-the-hood applications. Engine control units such as the turbocharger flap adjuster can be directly integrated with the mechanical systems.

Simple, PWM-based interfaces for motor control reduce the wiring harness to just a control wire and a power supply wire. Flexible, bi-directional control is made possible by bus concepts such as CAN or LIN. Conformity certificates and standard protocols make it possible to modularize beyond the various vehicle platforms. The additional development cost for electronics and software has been shied away from so far.

Principles of BLDC Motor Control

A BLDC motor consists of 3 coil phases rather than just 2 phases, as in a conventional DC motor.

These 3 coil phases are frequently switched to the supply voltage or ground potential; they also might be floating in between. This depends on the rotor position. Unlike the brushes in a conventional DC motor, commutation takes place electronically in this case. The required position detection to ensure proper commutation is often carried out using Hall sensors in sensor-based operation.

Systems without sensors are more and more being used as they are less expensive because there is no need for Hall sensors. Two concepts are basically available for operation without sensors. The back-EMK (back-electromotive force) measuring procedure requires less computing power than the second procedure, which is known as FOC (field-oriented current) method.

BLDC motor control electronics generally consist of the control part and the power stage (see figure 1). A microcontroller with PWM capability is needed for control purposes. The 3 half-bridges of the power stage are created using N-MOSFET switches.

The half-bridge switches (also called B6-bridge switches) are actuated using gate drivers. The upper power switches are another challenge. The control voltage of the upper switches must exceed the supply voltage. This is generated by a charge pump.

The control voltages also have to be available during voltage drops, e.g., when the vehicle is started. The functional operation has to be guaranteed down to 6V. Intelligent concepts such a dual-charge pump ensure that standard N-MOSFET switches are still reliably controlled using such low supply voltages. Standard MOSFETs have the advantage that their threshold voltage is still within a sensible working range, even at high ambient temperatures.

Other standard components of an ECU (electronic control unit) are the voltage regulator and the watchdog. The voltage regulator supplies the microcontroller and other digital components of the ECU with the appropriate supply voltage, whereas the separate watchdog monitors the microcontroller and the overall system. Automotive safety applications prescribe the use of a discrete monitoring circuit.

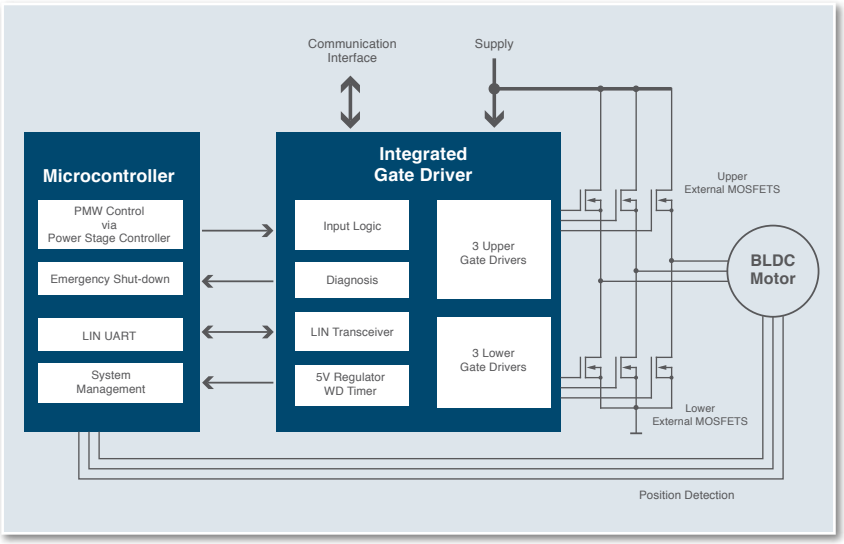

Figure 1. BLDC Control Block Diagram

Atmel's BLDC Motor Control Solution

Atmel provides an optimized solution that combines an AVR® microcontroller and an integrated gate driver, the ATA6833. The ATA6833 unites all of the control blocks that are needed for the BLDC control on a single IC: In addition to the 3 upper and 3 lower gate drivers, a voltage regulator, a watchdog and a LIN transceiver are integrated.

Integrated Gate Driver

The current capacity of the voltage regulator has been designed such that it can supply normal electronic units with up to 100 mA. The integrated run-time monitor provides the necessary system safety. Communication with the automotive environment is provided by a LIN transceiver from Atmel's well-known LIN family.

The gate drivers allow MOSFET switches to be used as lower and upper power semiconductors. A critical operating situation is the start-up of the vehicle. During the so-called crank pulses, the supply voltage drops considerably. However, a dual charge pump ensures that the external NMOS MOSFET switches are reliably opened. This charge pump provides an auxiliary voltage for actuating the MOSFETs via the supply voltage.

AVR Microcontroller

The ATmega32M1 is a member of Atmel's 8-bit AVR microcontroller family, which is characterized by its outstanding computing power and low power consumption. This microcontroller was specially developed for BLDC motor control applications in the automotive area.

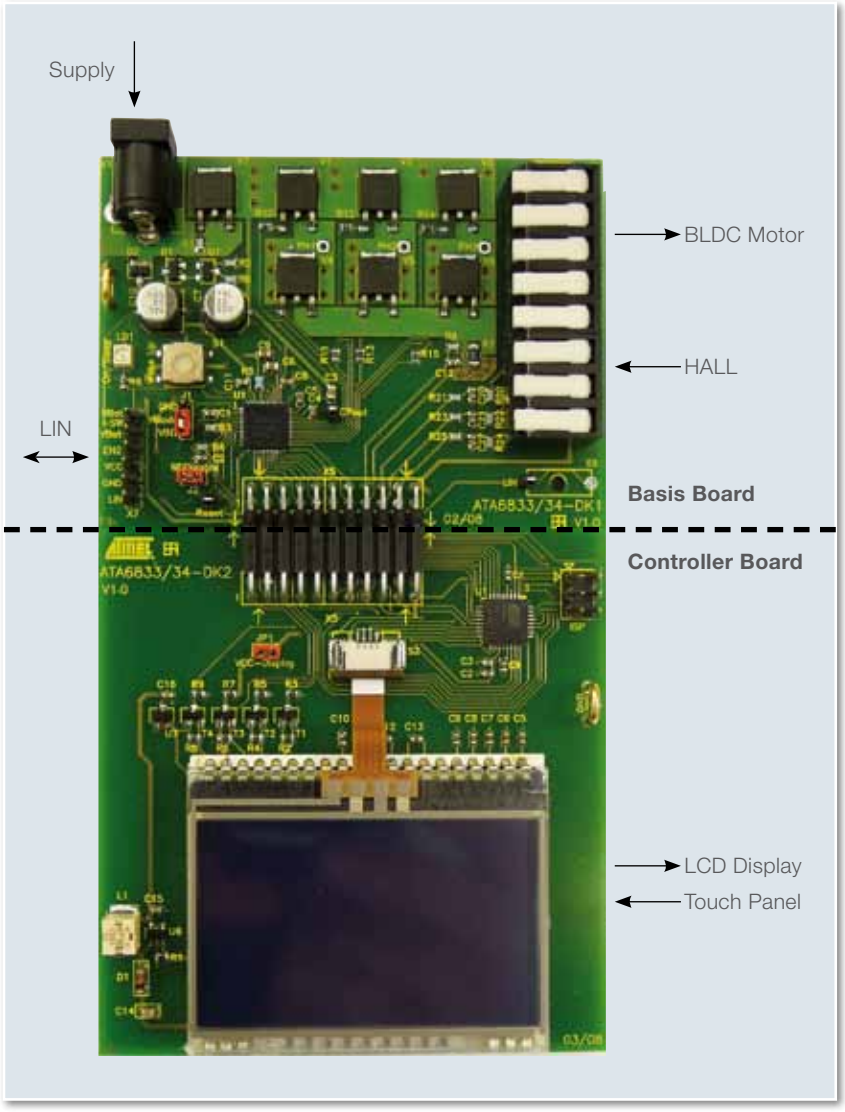

Figure 2. Application Board ATA6833-DK

As well as having 32k Bytes of Flash memory, this controller has 2k Bytes of SRAM and 1k Byte of EEPROM memory. A special feature is the integrated PWM generator, which is known as the “Power Stage Controller” (PSC). The PSC can generate up to 6 PWM signals with a resolution of 12 bits, which are needed for the three half-bridges of a BLDC motor control system. Up to 3 digital inputs or each output signal of the integrated analog comparators can influence PWM signal generation. This function can be used for emergency shut-offs or for current-controlled motor control. The ATmega32M1 also has an internal 8-MHz RC oscillator with a PLL that generates a frequency of up to 64 MHz, which serves as an input frequency for the PSC. Thus, PWM frequencies of up to 62.5k Hz can be generated with 10-bit resolution.

Other peripherals that are needed for a motor controller are available, such as an 8-bit timer and a 16-bit timer, a 10-bit ADC with up to 11 channels and a programmable preamplifier, a 10-bit DAC and 4 analog comparators. The controller provides a LIN interface and a CAN interface for communicating with the outside world.

High-temperature Capability

Both the ATA6834 and the ATmega-32M1 microcontroller are suitable for use in high-temperature environments. Both circuits are qualified in accordance with AEC-Q100 grade 0. This corresponds to an ambient temperature of up to 150 °C.

BLDC Application Board

The ATA6833 application kit shows the entire BLDC motor control chain from signal generation to signal amplification to the motor, and back again with position signaling. The kit consists of 2 units: The basic board with the power electronics, and the controller board with the microcontroller and the user interface.

The basic board is equipped with 6 MOSFETs for operating a BLDC motor. Only the commutation facility with Hall sensor feedback is supported. The digital encoding is done by the microcontroller, which also analyses the diagnostic signals and controls motor operation accordingly. The ATA6833’s integrated charge pump makes it possible to achieve reverse polarity protection with little voltage drop. This means that more powerful motors can be used.

The controller board, which is connected via a series of connectors, contains the microcontroller and the user interface.

The operating and diagnostic data are shown on a LCD display, which is also equipped with a touch panel as user interface. The provided software has implemented a simple LIN protocol. The system can therefore be remotely controlled using a basic set of LIN commands. In both cases, the BLDC motor can be conveniently controlled, operating states

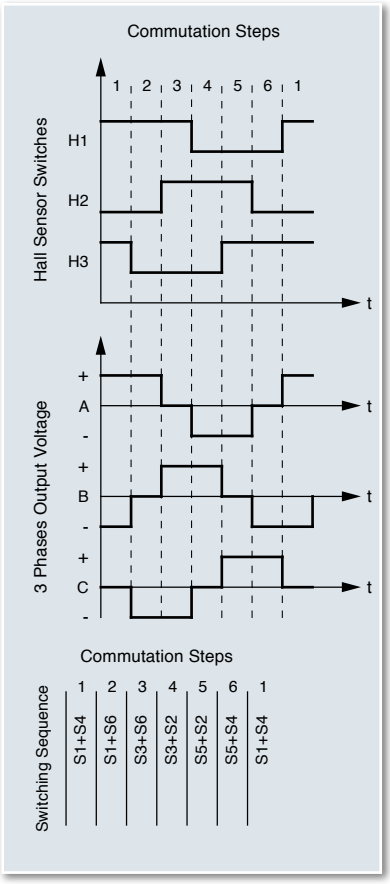

Figure 3. B6 Bridge Actuation

such as speed, direction, duty cycle and diagnostic states are displayed, and different methods to control the MOSFETs can be selected.

Actuation Procedure

Unlike mechanically commutated DC motors, the commutation of a BLDC motor must be performed electronically. This electronic commutation requires a specific switching sequence for all three half-bridges of the three coil phases (see figure 3). The switching sequence always depends on the rotor position, which is determined using Hall sensors, for example.

The simplest type of commutation for BLDC motors is block commutation. With this procedure, the coil amplitude remains stable during one communication step. A somewhat more complicated method is sinusoidal commutation, whereby the amplitude is modulated in such a way that sinusoidal current flow is generated by the respective coil phase. Figure 4 shows both methods.

The advantage of sinusoidal commutation is the harmonic actuation sequence, which reduces vibration and the resulting amount of noise, which is much higher when using block commutation because of the "hard" switching sequence. The disadvantage of the sinusoidal commutation procedure is complexity during implementation and the amount of microcontroller computing power that is required, whereas block commutation is quick and easy to realize.

For simplicity's sake, block commutation has been used in the ATA6833 application kit.

As well as the different commutation methods, other methods of actuat-

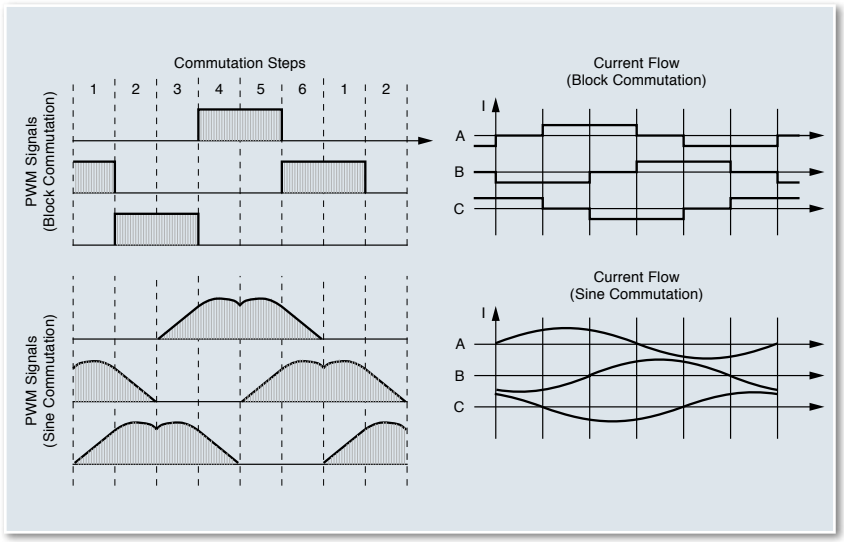

Figure 4. Sine Wave versus Block Commutation

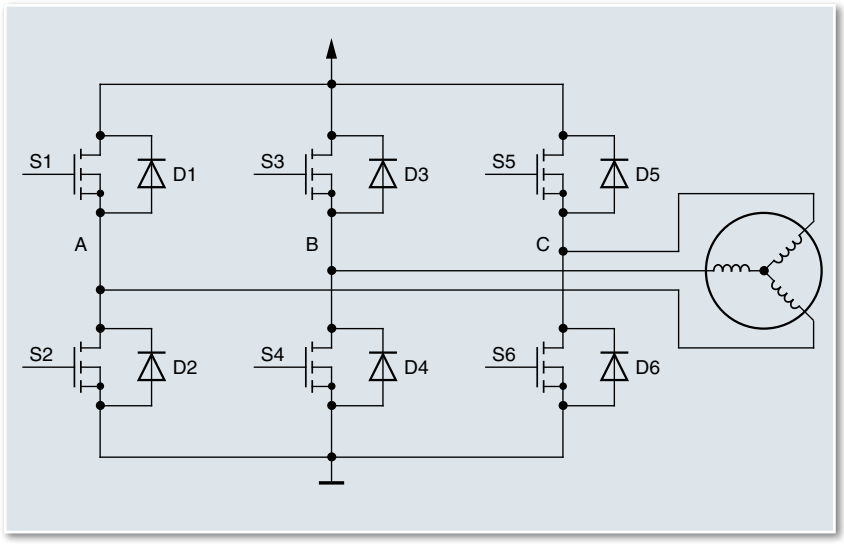

Figure 5. B6 Bridge

ing the B6 bridge are also available, i.e., two-quadrant and four-quadrant switching mode.

With the two-quadrant switching procedure, phase A is permanently switched to a potential, whereas phase B is switched to the opposite potential using a PWM signal. An example can be seen in figure 5: If switch S4 permanently switches phase B to ground, switch S1 clocks phase A to the supply voltage. This is so-called high side clocking. However, S1 can also be permanently switched through to the supply voltage, whereas S4 clocks to ground potential (low side clocking). The duty cycle of the PWM signal determines the current flow through the coil and consequently also the torque of the motor.

When the synchronous four-quadrant switching scheme is used, switches S1 and S4 are clocked simultaneously (high-side and low-side clocking).

The advantage of this method compared to the one described above is the quick change of rotating direction, whereas less switching loss occurs with the two-quadrant switching method. The disadvantage of both methods is power loss and the resulting intrinsic heating of the MOSFETs that occurs during the blocking phase of the PWM signal. The motor is idling at this time; the continued rotation of the rotor induces current in the motor coil, which flows through the freewheeling diodes of the MOSFETs.

To reduce this power loss, the MOSFET whose freewheeling diode is loaded is switched through during the blocking phase of the PWM signal. An example (see figure 3) in two quadrant chopper operation with high-side switching: Switch S4 permanently switches phase B to ground, and switch S1 switches phase A to the supply voltage in a clocked manner. During the blocking phase of the PWM signal of switch 1, a current is generated in the motor coil that flows through diode D2. In order to now relieve diode D2, switch S2 is switched through during the blocking phase. Switch S2 is now actuated with the inverter PWM signal of switch S1.

This procedure can also be used during four quadrant chopper operation by always actuating switches S2 and S3 with the inverted PWM signal of switches S1 and S4. This method is known as simultaneous, complementary 4 quadrant switching.
The motor actuation of the ATA6833 application kit can operate using either two-quadrant or four-quadrant switching operation, but the procedure for relieving the freewheeling diodes is only supported in two-quadrant switching operation.

More detailed motor control information can found on Atmel's website at:

AVR motor control	http://www.atmel.com/products/AVR/mc/?family_id=607
Application Note	http://www.atmel.com/dyn/resources/prod_documents/doc9143.pdf
BLDC Driver	http://www.atmel.com/dyn/products/product_card.asp?part_id=4412

Standard Products

Networking

LIN

Switch Matrix Module Design Using LIN SiPs ATA6612/13

Markus Schmid

Introduction

The LIN bus is well established in automotives where it is used for low-cost and low-speed applications as an alternative to the CAN bus. The implementation of the LIN bus is still increasing: in 2011 there are approximately 600 million LIN transceivers expected in all cars worldwide, and in 2014 this number is set to increase to 900 million.

The popularity of LIN devices can in part be attributed to their flexibility: they can be used in many different applications. Typical LIN applications either evaluate the data of sensors or switches or drive actuators like motors or a heating system. However, those LIN applications must not have high-speed or even real-time requirements. Therefore, LIN devices can be found in window lifts, mirrors, or keypads in car doors. They are also used in seat heating or adjustment, in climate control, in the dashboard or for wiper control, where LIN is currently the unchallenged standard.

The expected increase in the amount of LIN devices in the coming years can be explained by the continued requirement for comfort functions in next-generation automotives. As almost all comfort functions can be controlled by the passengers via keypads, it is expected that the amount of the keypads will also increase. This article covers efficient keypad evaluation using a switch matrix module.

LIN SiPs ATA6612 and ATA66613

The ATA6612/13 consists of two chips in a single package; the first one is the LIN system basis chip (LIN SBC) ATA6624, which has an integrated LIN transceiver, a 5V voltage regulator, and a window watchdog. The second chip is an AVR® 8-bit RISC automotive microcontroller. The ATA6612 consists of the LIN SBC ATA6624 and the ATmega88 with 8-kBytes flash, while the ATA6613 includes the ATA6624 and the ATmega168 with 16-kBytes flash. The only difference between the two microcontrollers is the size of the Flash memory. All pins of the LIN System Basis Chip as well as all pins of the AVR microcontroller are bonded out so that the customers can use the well-established AVR tools. It also provides the same flexibility for the applications as when using the discrete parts.

Handling Keypads

The easiest way to evaluate a push button is to connect it directly to an I/O pin of a microcontroller. This is the preferred solution, when only a couple of push buttons need to be evaluated by a single microcontroller. But with an increasing number of switches, the number of I/O pins increases accordingly. In many cases this leads to a need for larger and therefore more expensive microcontrollers. Using a switch matrix the number of I/O pins required can be reduced. Using a 3 x 2 matrix up to six push buttons can be monitored using only five I/O pins. With the conventional solution where a single push button is connected to one I/O pin, only five push buttons can be evaluated. With more push buttons, a switch matrix will lead to even greater savings in the number of I/O pins required. For example, a 3 x 3 matrix can handle up to nine

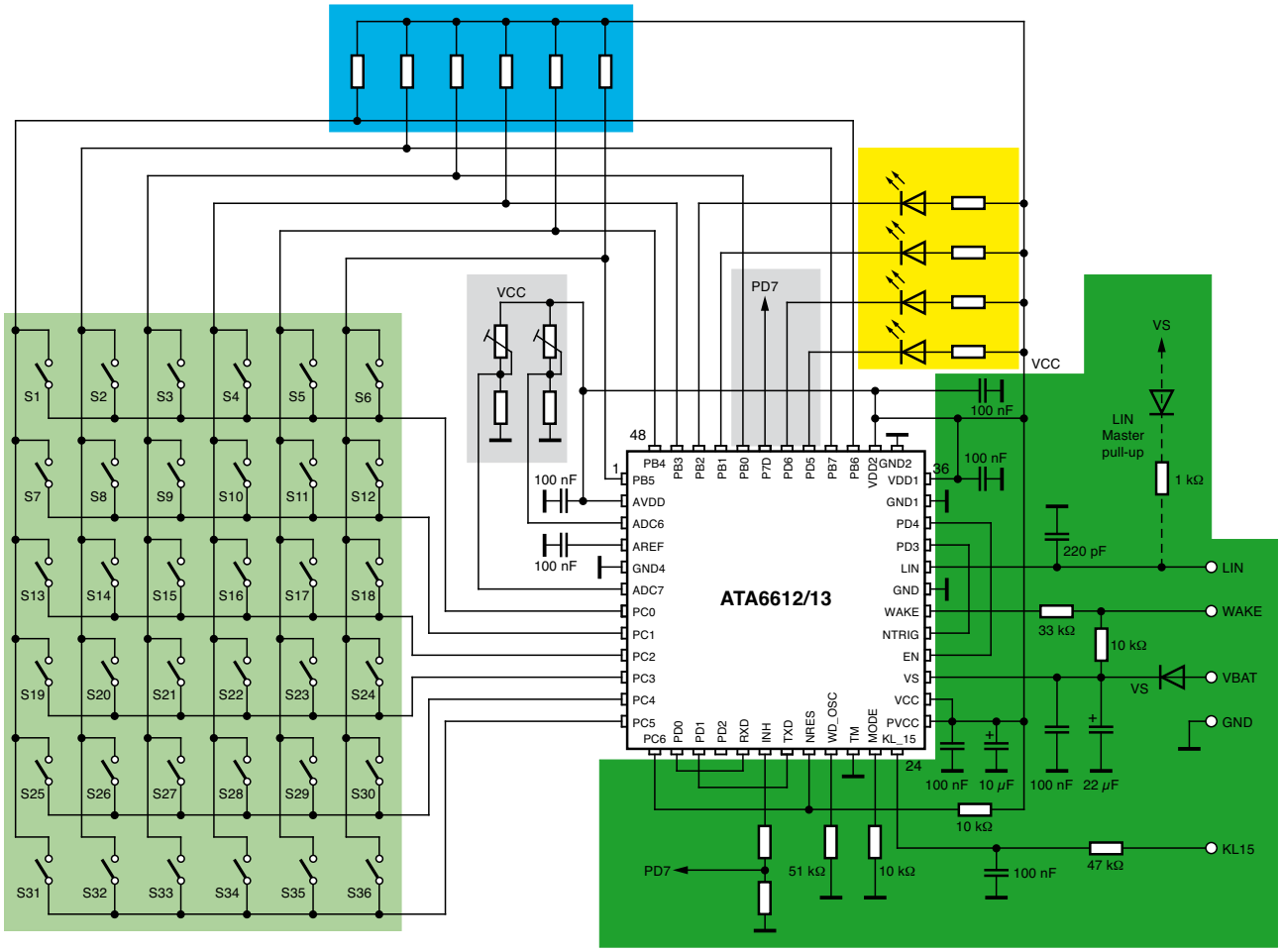

Figure 1. Switch Matrix Application

push buttons with six I/O pins leading to a saving of three I/O pins compared to the single push button per I/O pin solution.

Switch Matrix Using LIN SiPs ATA6612/13

Figure 1 illustrates an application that can be commonly seen in climate control panels. It shows a switch matrix serving some additional requirements.

The keyboard matrix is organized in 6 x 6 push buttons (light green area), which enables the ATA6612/13 to handle up to 36 push buttons. That is a very large number of push buttons, but it can be easily reduced by removing columns or rows. In general, pressing a key connects the key's row and column lines. When pressing the top left key, the left-most column line is connected to the top-most row line. The microcontroller can detect this connection by scanning the columns and rows. When only single keys are pressed, a quick method is to first select (drive low) all row lines and read the column result. Then all column lines are selected, and the row result is read. Returned column and row values are combined into a unique scan code for the specific key pressed. When the detection of simultaneous key presses is required, this method has to be slightly changed. The rows must be scanned separately. The row lines must be driven low sequentially, reading the column result for each row, thus getting all pressed keys.

The illustrated pull-up resistors in the light blue area are very important for the scan algorithm to monitor the push buttons. These do not necessarily have to be external resistors; however, as internal resistors are very high ohmic and many applications need to have a higher current through a closed push button; it is common to add more low-ohmic, external resistors allowing a higher current to flow. Using only the internal pull-up resistors of the AVR will lead to a current of approximately 160 µA through the pressed keys.

Almost all keypads in a contemporary car have the ability to switch on a backlight in order to illuminate the push buttons. This enables the passengers to find the desired key even in a dark environment. The backlight illumination consists of several LEDs, whose brightness can be varied when they are controlled by a PWM pin of the microcontroller. In the schematic, the four LEDs in the yellow area are connected to the PWM pins PB1, PB2, PD5 and PD6. In general, the ATA6612/13 has up to six PWM pins.

In addition to the backlight illumination in an automotive keypad, there are very often rotary encoders to be evaluated by the microcontroller which also controls the evaluation of the keypads themselves. Shown in figure 1 as two variable resistors in the gray area, which can be evaluated using two of the available eight ADC channels. As the resistors are connected to the supply voltage in this example, it is best to also use the supply voltage as reference voltage for the conversion. It is also possible to choose a fixed internal 1.1V or an external reference voltage between 1.0V and the voltage connected to the AVCC pin of the microcontroller. In addition, pin PD7 serves as an input for an analog-to digital conversion. It is connected via a voltage divider to the INH pin. Therefore, the module's battery voltage in standard operation mode can be monitored very efficiently. In current save mode the current consumption does not increase since the INH pin will be switched off in this mode.

The other external circuitry in the dark green box in the schematic are blocking capacitors for the microcontroller or, as the INH pin, relevant for the features of the LIN part. The resistor connected to the WD_OSC pin, for example, is important as it adjusts the watchdog frequency of the internal window watchdog. The circuitry connected to the WAKE, KL_15, and the LIN pin is optional and can be adjusted to the needs of the application.

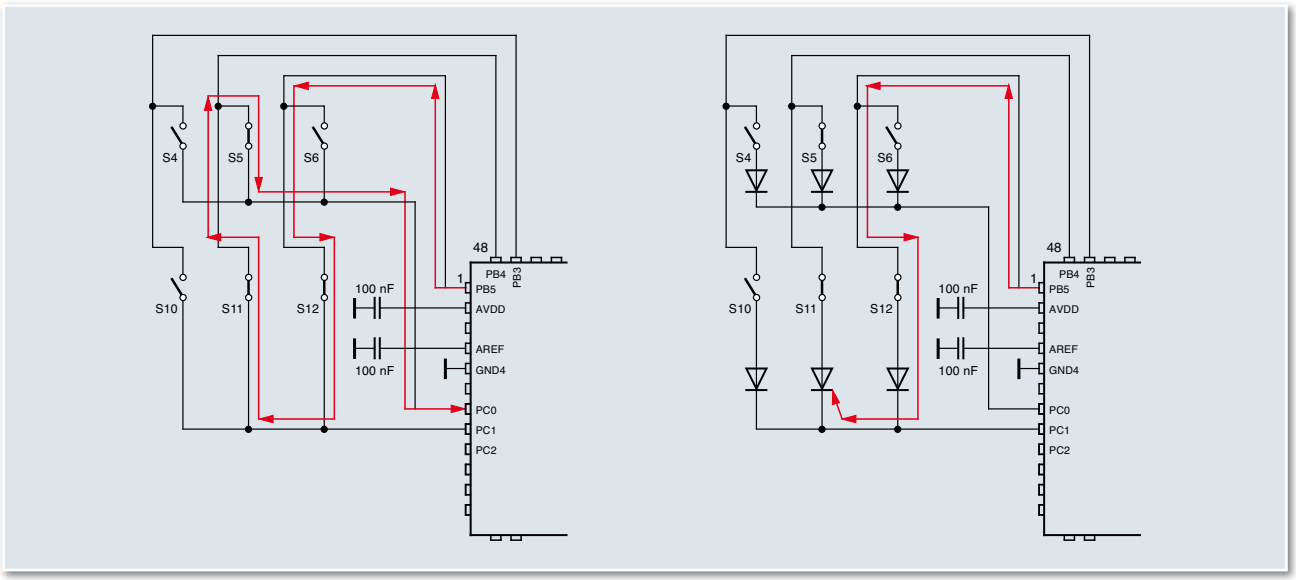

Figure 2. Current Flow During Simultaneous Key Presses

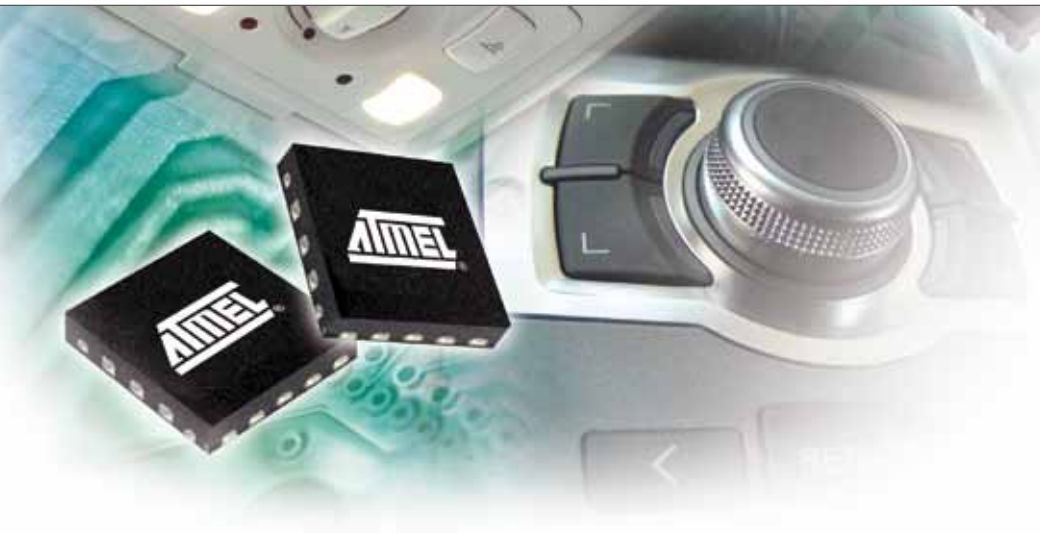

Detection of Simultaneous Key Presses

Some additional hardware precautions must be taken when detection of simultaneous key presses is required. The schematic as shown in figure 1 may lead to erroneous results, which is explained in the following.

If the keys S5, S11 and S12 are pressed at the same time, the microcontroller will determine that key S6 is also pressed, although this is not the case. The current, which flows when the three keys S5, S11 and S12 are pressed, is shown in figure 2 in red. The microcontroller can not distinguish whether the three pins are pressed or if the key S6 is pressed. In order to avoid this behavior an additional diode has to be included at every key which stops the undesired current flow and enables to achieve the correct result. Using these diodes prevents undesired result. Shottky diodes are preferable as they have a lower forward voltage compared to normal diodes.

Current Consumption

Current consumption is, as in all electronic modules in cars, a key parameter for the switch matrix. A current consumption limit of 100 µA in silent mode is the most common requirement, which is met by the ATA6612/13. The ATA6624 has two different current saving modes. The first is the sleep mode, which shuts down the watchdog, the LIN transceiver as well as the voltage regulator. Thus, the microcontroller remains currentless in sleep mode and it is not possible to continue to scan the keys. The ATA6612/13's typical current consumption in sleep mode is 10 µA. The second current saving mode is the silent mode. In this mode the watchdog and the LIN transceiver are switched off, but the internal voltage regulator remains active, thus allowing the microcontroller to continue to scan the keys. The ATA6624's typical current consumption in this mode is 57 µA. The ATA6624 can wake-up via a message on the LIN bus or via an event at the pins WAKE or KL_15. In order to achieve the 100 µA limit, the microcontroller must switch itself into a current saving mode. The ATmega88/168 offers five different current saving modes with different active components and wake-up sources. To continue to scan the keys, the user should choose a power-saving mode with a cyclic wake-up. After recognizing a pressed key, the microcontroller can then wake-up the ATA6624 as well as the complete LIN network, and start the transmission of this event via the LIN bus after a master request. With this set-up, no event will be missed even in power-saving mode.

Conclusion

The ATA6612/13 is a perfect choice for applications where many keys have to be monitored and the key press events have to be transmitted via the LIN bus. Figure 1 illustrates how such a module can be built. However, in many cases it is necessary to adapt to the special needs of a particular matrix. The ATmega88/168 included in the ATA6612/13 is a standard microcontroller, therefore, the extensive application notes related to the ATmega88/168 can also be used for the ATA6612/13.

Application notes Atmega88/168 see
http://www.atmel.com/dyn/products/product_card.asp?family_id=607&family_name=AVR%26reg%3B+8%2DBit+RISC+&part_id=3757 and
http://www.atmel.com/dyn/products/product_card.asp?family_id=607&family_name=AVR%26reg%3B+8%2DBit+RISC+&part_id=3758

Standard Products

Networking

LIN

LIN Node Mirror Positioning and Folding

Rainer Boehringer

Modern wing mirrors incorporate a variety of functions. Previously managed manually, bi-axial positioning was the first feature to be automated. Recent advancements include a memory function where different mirror positions are stored. With this memory function, when reverse gear is engaged the mirror automatically repositions from a driving position to a parking position.

With the motor-foldable mirror, the mirror can be brought into an operating position or into a folded-in position in which the mirror is less susceptible to accidents. Operating circuitry enables a motor to be activated by a switch, preferably by applying a voltage across the motor with a polarity dependent on the desired direction of rotation of the motor.

In addition to the basic function of mirror heating, side mirrors also boast many additional safety and convenience features including electro-chromatic blank off, entrance lamps, direction indicator, antenna systems, distance warning, or sensor systems for modern traffic management systems. To control functions like heating or chromatic blank off, ON/OFF switches are sufficient. These functions can

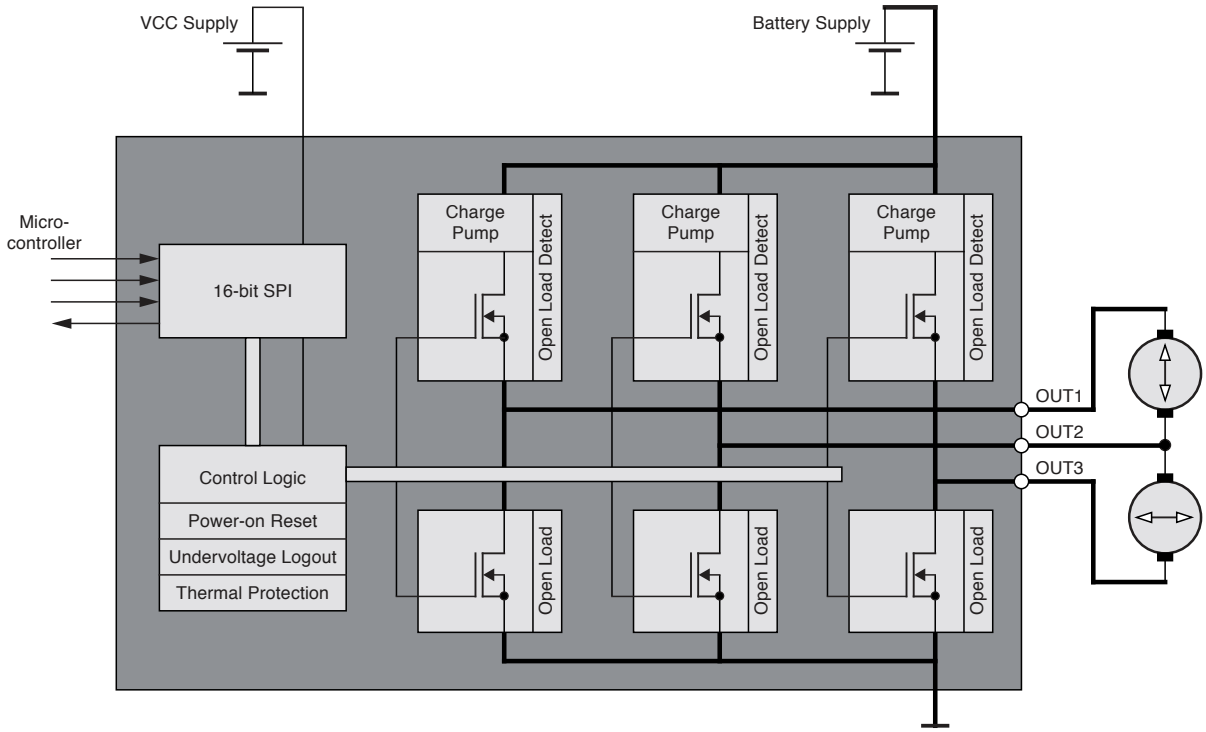

Figure 1. ATA6826 Block Diagram

be activated via external MOSFETs directly controlled by a microcontroller. To control movement functions such as positioning and folding, more intelligence is necessary and smart drivers are required.

Part No.	Minimum Short-circuit Current	Thermal Resistance Junction – Ambient
ATA6826	1A	65 K/W
ATA6827	1A	40 K/W
T6818	1.5A	65 K/W

Table 1. Triple Half-bridge Output Driver Overview

Drivers for Positioning Control

Mirror positioning is accomplished using DC motors which require advanced control. Integrated circuits are typically designed as triple half bridges to be configured as two H-bridges. Two H-bridges are necessary to control two DC motors for the two-axes positioning of a rear mirror. The half bridges are each combined with two save-spacing NMOS MOSFETs. To control the upper MOSFETs as NMOS, three independent charge pumps are integrated. Due to their asynchronous operation and that they switch on only during a HS switch on, better EMC performance is achievable (see figure 1).

As these devices are fully protected against short circuits and overtemperature, connection of DC motors without any additional protection circuitry is possible. Open-load detection is also available to check the electrical connection of the motors: during activated state of the outputs, the drivers feedback whether a DC motor is connected or not.

The ATA6826 is able to drive DC motors up to 1A. Under normal circumstances, this is sufficient for mirror positioning systems. For higher performances, the T6818, which is capable of driving currents up to 1.5A, can be used (see table 1).

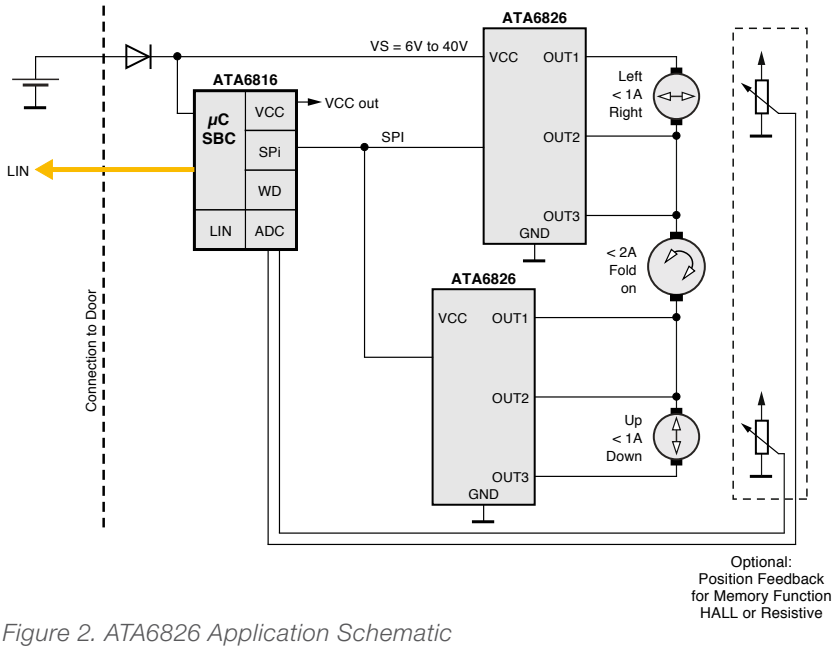

Figure 2. ATA6826 Application Schematic

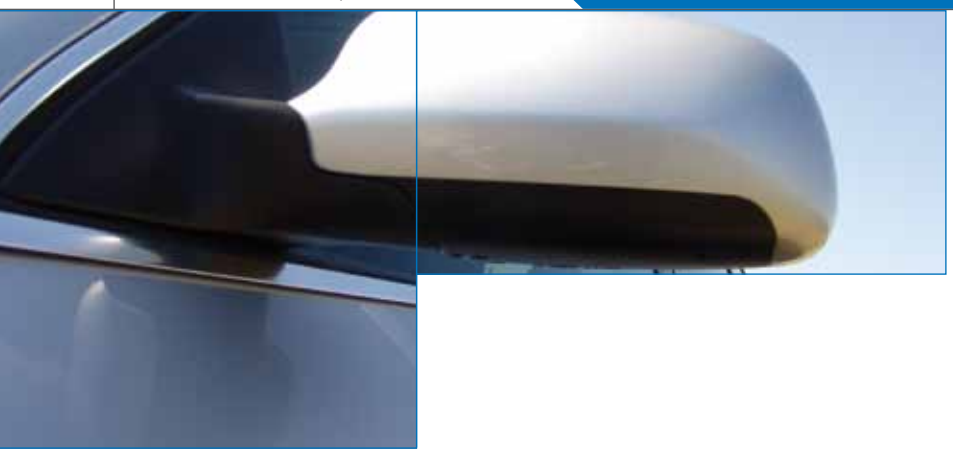

For motor-foldable mirrors, a current capability of about 3A is necessary. To meet this requirement, two half-bridge outputs can be combined to achieve double output current (see figure 2). A feature of the NMOS output stages is the positive thermal sensitivity shift. At higher temperatures, the outputs' resistance increases. The current of the two combined outputs is automatically balanced.

Mirror folding causes higher power dissipation due to the higher current. When using two triple half-bridge drivers in the configuration as shown in figure 2, the power dissipation is shared between the two devices. The benefit of this set-up is the distribution of the power dissipation between two sources.
Stall condition and end stop are a challenge for the mechanical positioning system. Usually, the blocking currents of the DC motors are in the same range as the operating currents of the motors. The output driver cannot distinguish between operating and blocking condition. As a motor-safety function, side mirrors are equipped with slipping clutches. And as such, there is no need to measuring the DC motor current. Security switch-off is protected by the clutches.

More advanced side mirrors can be equipped with a memory function. With this function, the system requires feedback on the position. An additional potentiometer or angle sensor is required. By measuring and storing the various mirror positions, these can be simply adjusted again. Due to the increasing number of DC motors for seat, steering and mirror adjustment, the memory function is getting more and more important.

Door LIN Node

As the number of features and functions increases, so too does the number of control lines, which results in an increasingly complex harness. To reduce this complexity, a certificated bus system is indispensable. The use of a single-wire LIN bus reduces the wiring to a minimum. Integrating voltage regulator, LIN transceiver, and microcontrollers, Atmel's LIN SIPs include all the required units to complete the basic functions of an ECU to control a side mirror (see figure 2).

Figure 4 shows the integration of mirror node and LIN cluster in the door electronics. In addition to the mirror control node, the block diagram shows a node for window lift and a node for the switch unit.

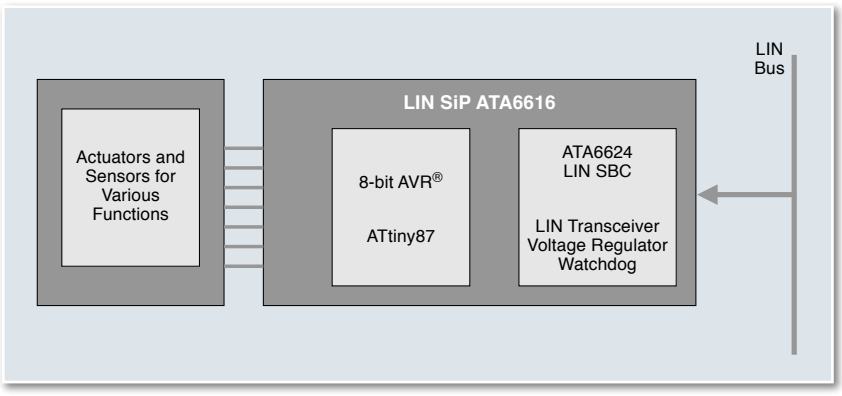

Figure 3. Block Diagram LIN SBC ATA6616

The control unit can be carried by a single device, a LIN SiP (see figure 3). The control of a switch matrix enables the scanning of all the different user buttons.

The window lift module can completed using two devices: Atmel's ATA6823 H-bridge pre-driver with LIN transceiver, voltage regulator and watchdog to manage the supply and interface part; and Atmel's ATtinyxx microcontroller with its integrated LIN UART for LIN protocol handling and movement control including the anti-pitch algorithm.

Package

All these functions need to fit into the casing of a side mirror. And depending on vehicle variants, even more functions will be added. Atmel's mirror solution enables manufacturers to use one basic system with a high rate of flexibility, allowing adding further features that can be produced via assembly variants. As all Atmel devices are available in very small QFN packages, these drivers and LIN SIPs can facilitate even the tightest designs.

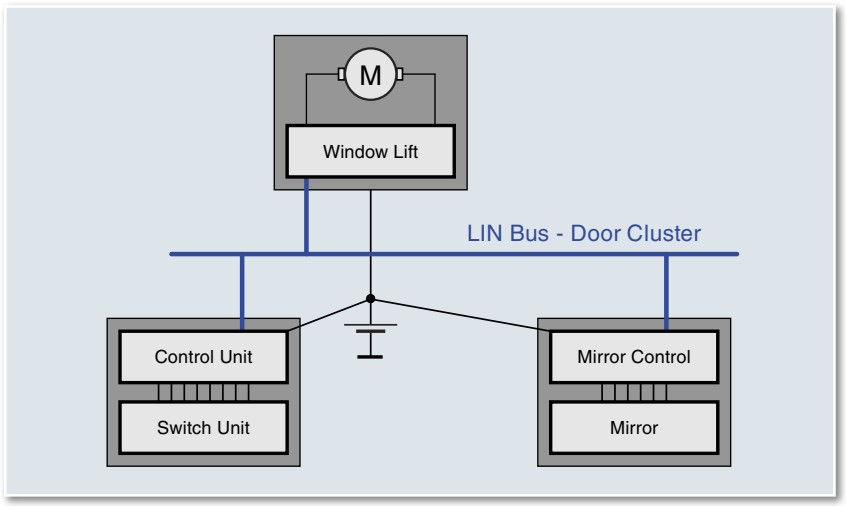

Figure 4. System Diagram Door LIN Cluster

Appendix

For further information see

Atmel Driver ICs
http://www.atmel.com/products/drivers/default.asp
Atmel LIN Networking
http://www.atmel.com/products/lin/default.asp
Atmel's Automotive Microcontrollers
http://www.atmel.com/dyn/products/devices.asp?family_id=690
Application Note LIN Node Mirror Positioning and Folding
http://www.atmel.com/dyn/resources/prod_documents/doc4946.pdf

Standard Products

Development Platform Evaluation Kit for Automotive Applications

Juergen Strohal, Karl Militzer

With automotive applications, the increasing level of integration on the chip side demands a corresponding increased effort on the application tool side. While customers, in general, do not like dealing with different stand-alone tools for each new application, there is an increasing need to evaluate complete sub-systems. Atmel's new automotive application development kit, ATAPMxx addresses these needs. This is a tool that helps customers not only to develop their application but also to evaluate application performance in a single environment. It is flexible and modular, and allows easy extension for new devices. All former tools from the car access area have been integrated into this new kit. Together with the upcoming AES devices Atmel is able to offer a system that can set up a complete Remote Keyless Entry (RKE) or a Passive Entry/Go (PEG) application for both the car and the key side. This kit is also currently being expanded to include LIN networking capabilities so that the evaluation of complete LIN bus product portfolio – standard transceivers and system basis chips as well as LIN system-in-package solutions – is supported.

The new evaluation kit is a modular, flexible application system to support customers in developing and evaluating their new applications. However, does flexible also mean complicated and cumbersome to use? Not with Atmel! The ATAPMxx was also designed to be easy-to-handle. "Out of the box" operation was one of the main development goals. Customers familiar with the former car access application tool "RF design kit" do not need to relearn completely new operation software as a nearly identical user interface is also supported by ATAPMxx. The system offers the hardware and software to develop and demonstrate complete system solutions. Hardware and software documentation serves as a useful starting point for customers' development.

The development kit comprises a main board as well as a selection of application and daughter boards, depending on the designated application. The most important part is the main board ATAPMMB with system controller, LCD display and touch screen, USB interface for PC connection, two-wire-serial interface (TWI) as connector for various application boards, an SD card slot, power supply connector, and a beeper. While the daughter boards function as RF transmitter or transceiver, the application boards act as an interface for the daughter boards to the system's two-wire serial bus. The main board can manage and control a complete application with different daughter boards as a stand-alone system. This is particularly useful if customers need to conduct a brief evaluation of functions and performance, or if a ready-to-run demonstrator is needed, which does not require a complex set-up procedure.

For more elaborate evaluation, the main board can also be used as an interface to a PC. Using the PC-based GUI, the system performance can be evaluated in all details, new configurations can be downloaded to certain components, and received or transmitted data can be displayed. The board is powered by an AT90USB128 AVR® microcontroller which serves as USB connection to the PC, and handles the touch panel and the communication with the application boards that are connected via the TWI.

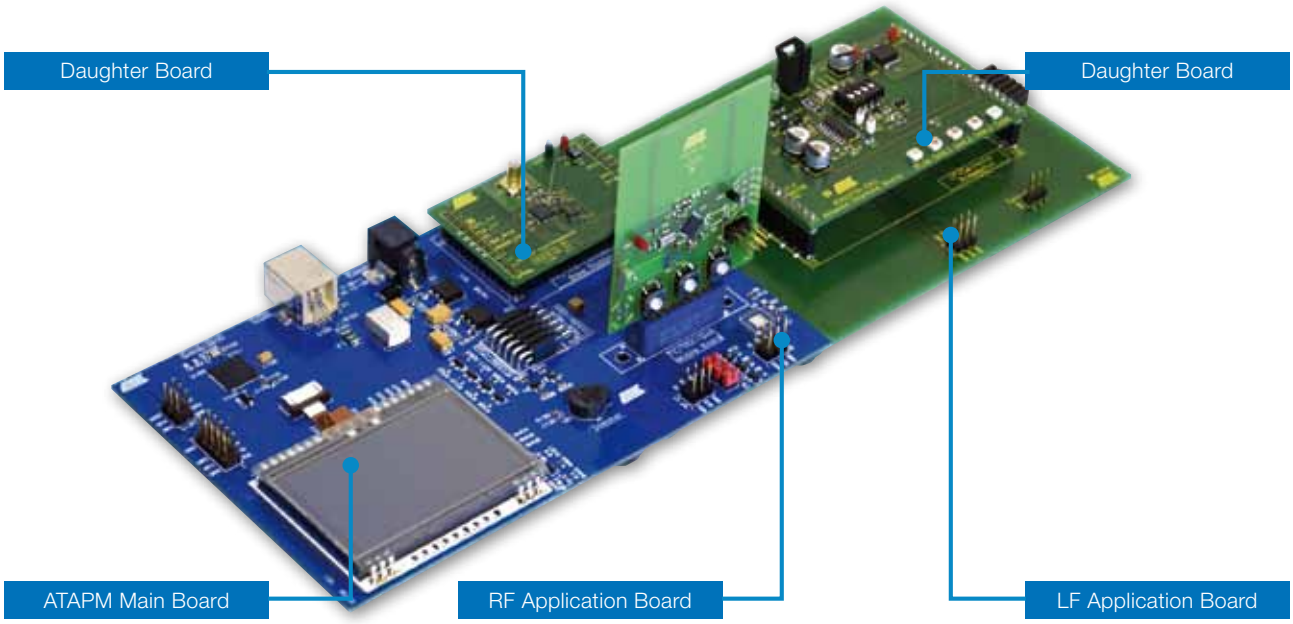

As shown in figure 1, a number of different application boards are available. These boards carry the daughter boards for the required application and are equipped with TWI connectors on both ends so that practically an unlimited number of application boards can be attached in a row to a single main board. The standard RF application board contains its own AVR microcontroller (ATmega168) to handle the RF application as well as the communication to the main controller on ATAPMMB. Various daughter boards can be connected via two rows of connectors on top of the application board. A wide variety of daughter boards with RF receivers or transceivers are already available from the well-known RF design kit, and the number of boards continuesly grows. An additional connector can also be used to attach a transmitter or transceiver board for configuration purposes. This can be disconnected from the RF application board once it is configured and can operate as a battery-powered mobile device.

Some functions in remote keyless entry or passive entry (go) applications such as authentication/ immobilizer, system wake-up or inside/ outside detection of the key are often realized by LF links. The LF application board that supports these functions is quite similar to the RF application board, it contains its own microcontroller (ATmega168), which is responsible for the application and the communication with the main board via two-wire-serial interface. Currently, the LF application board supports two different functionalities, depending on the attached daughter board; it can operate as immobilizer base station (powered by U2270B), or it can be used in a PEG application with a 6-fold antenna driver (ATA5279).

To create a complete application, the appropriate parts and corresponding boards must be selected. For example, to design a bi-directional PEG system with RF/RF-authentication channels, a mobile board with the new, upcoming AES IC plus ATA58xx transceiver used as “key” are required. In addition, the main board, an RF application board, and two LF application boards plus two LF daughter boards are also needed. The main board and application boards – equipped with the appropriate daughter boards and plugged together via TWI – represent the “car” side of the system. Other configurations with mixed

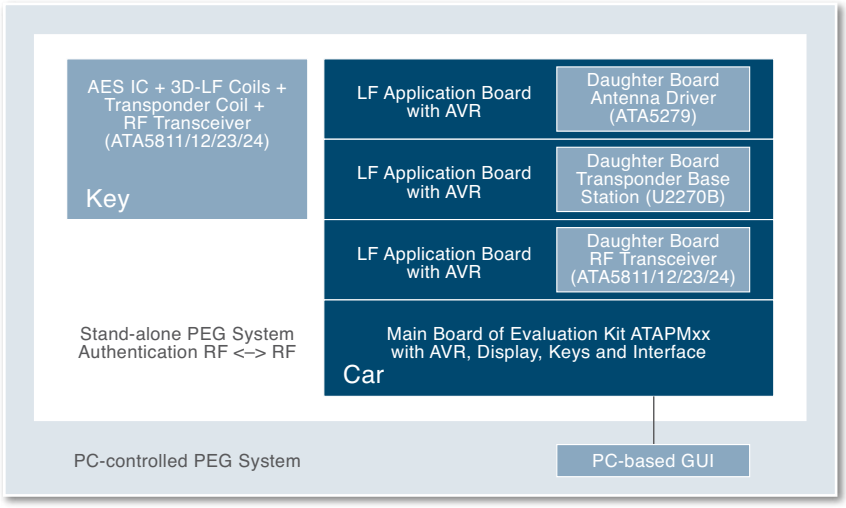

Figure 2. System Hardware Configurations for PEG

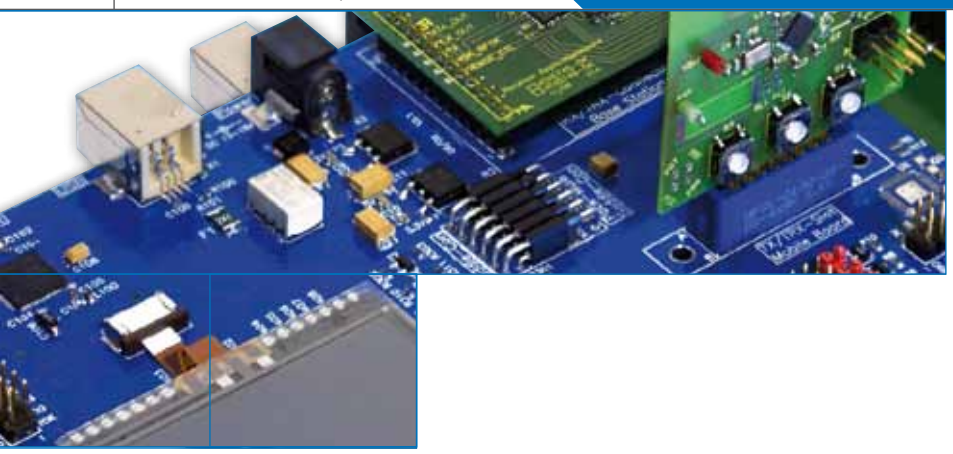

RF/LF authentication channels are also possible.

While the new application platform incorporates a fully modular concept so that can be freely configured according to individual needs, Atmel also offers a number of fixed configurations for applications that are requested more frequently, for example, remote keyless entry or passive entry go systems. These fixed configurations facilitate to address certain applications without the need to study selection guides or to get familiar with the details of the ATAPMxx development platform. They are an ideal starting point for newcomers, yet still offer full flexibility in that they can be extended or adapted to other application needs at any time by simply ordering additional components.

The ATAPMxx has exhibited at the Automotive Electronic Show in Shanghai in April 2009 where it

		Content of Pre-configured ATAPM System Kits for Remote Keyless Entry						
Part Number of Single Boards \ Complete Kits ➡ ⬇		RF 1-way			RF 2-way		RKE1	
	Comment	ATAPMRF11-DK1	ATAPMRF12-DK1	ATAPMRF13-DK1	ATAPMRF21-DK1	ATAPMRF22-DK1	ATAPMRKE1-DK1	ATAPMRKE2-DK1
Automotive Evaluation Kit System Controller								
ATAPMMB-DK	ATAPM main board	LCD, touch screen, USB-AVR, interface to PC & application	ATAPMMB-DK	ATAPMMB-DK	ATAPMMB-DK	ATAPMMB-DK	ATAPMMB-DK	ATAPMMB-DK	ATAPMMB-DK
Application Boards								
ATAPMRFS-DK1	RF application board	Standard for RKE & PEG	ATAPMRFS-DK1	ATAPMRFS-DK1	ATAPMRFS-DK1	ATAPMRFS-DK1	ATAPMRFS-DK1	ATAPMRFS-DK1	ATAPMRFS-DK1
ATAPMLFS-DK	LF application board	For immobilizer base station & 3D-LF base station						ATAPMLFS-DK	ATAPMLFS-DK
RF Daughter Board with								
ATA5745/46-EK	ATA5745/46	RF-Rx						ATA5746-EK	ATA5745-EK
ATAB5760-S	ATA5760	RF-Rx with SAW filter			ATAB5760-S				
ATAB5761-N	ATA5760	RF-Rx							
ATA5723/24-DK	ATA5723/24	RF-Rx	ATA5723-DK	ATA5724-DK	ATA5724-DK				
ATAB5811/12-B	ATA5811/12	RF-TRx				ATAB5812-B	ATAB5811-B		
ATAB5823/24-B	ATA5823/24	RF-TRx							
LF Daughter Board with								
ATA2270-EK2	U2270B	Immobilizer base station							
ATAB5279	ATA5279	6-fold LF antenna driver							
Mobile Parts with								
ATAB5753/54	ATA5753/54	RF transmitter for RKE	ATAB5753	ATAB5754					
ATAB5756/57	ATA5756/57	RF transmitter for TPMS							
ATAB5749	ATA5749	RF transmitter for RKE							
ATAB5811/12-RS	ATA5811	RF transceiver for remote start				ATAB5812-RS	ATAB5811-RS		
ATA5771/73/74-DK1	ATA5771/73/74	Tx-MCM			ATA5771-DK1				
ATA5795-EK1	ATA5795	for RKE incl. Transponder function						ATA5795-EK1	ATA5795-EK1
ATA5790-EK1	ATA5790 + TX ATA5749	for PEG using RF/LF-authentication link							
ATA5790-3/-4-EK2	ATA5790 + TRX ATA5823/4	for PEG using RF/RF-authentication link							

Table 1. Complete Configuration for Remote Keyless Entry Applications

served as the heart of a demonstrator for a remote keyless entry and immobilizer system. This development platform, however, is not restricted to applications in the car access application field. While its current applications target the car access market (remote keyless entry, passive entry/go, immobilizer, and remote start), the next steps involve additional functions such as LIN bus connectivity, high-voltage systems and further configurations of existing application boards and daughter boards. Currently, Atmel provides several well-accepted stand-alone development tools for LIN transceivers, system basis chips and system-in-package (SiP) ICs as well as development boards and kits for a variety of Atmel's load drivers. Due to the advance of LIN SiPs and the need to cross-link different electronic control units it is useful to bridge LIN and car access systems. Therefore, a dedicated LIN application board will be available within short. This board, together with the main board, will convert the kit into a LIN master node with minimum effort as the basic software routines are bundled with the LIN board. In addition, the integration of the load driver family into this development platform will enable the evaluation of complete door modules.

All kits come along with a selection guide, descriptions of hardware and software, software library functions, and guidelines for system set-up.

			Content of Pre-configured Complete ATAPM System Kits for Passive Entry Go Application			
Part Number of Single Boards \ Complete Kits ➡ ⬇			PEG1		PEG2	
		Comment	ATAPMPEG-DK1	ATAPMPEG-DK2	ATAPMPEG-DK3	ATAPMPEG-DK4
Automotive Evaluation Kit System Controller						
ATAPMMB-DK	ATAPM main board	LCD, touch screen, USB-AVR, interface to PC & application	ATAPMMB-DK	ATAPMMB-DK	ATAPMMB-DK	ATAPMMB-DK
Application Boards						
ATAPMRFS-DK1	RF application board	Standard for RKE & PEG	ATAPMRFS-DK1	ATAPMRFS-DK1	ATAPMRFS-DK1	ATAPMRFS-DK1
ATAPMLFS-DK	LF application board	For immobilizer base station & 3D LF base station	2xATAPMLFS-DK	2xATAPMLFS-DK	2xATAPMLFS-DK	2xATAPMLFS-DK
RF Daughter Board with						
ATA5745/46-EK	ATA5745/46	RF-Rx			ATA5746-EK	ATA5745-EK
ATAB5760-S	ATA5760	RF-Rx with SAW filter				
ATAB5761-N	ATA5760	RF-Rx				
ATA5723/24-DK	ATA5723/24	RF-Rx				
ATAB5811/12-B	ATA5811/12	RF-TRx				
ATAB5823/24-B	ATA5823/24	RF-TRx	ATAB5823-B	ATAB5824-B		
LF Daughter Board with						
ATA2270-EK2	U2270B	Immobilizer base station	ATA2270-EK2	ATA2270-EK2	ATA2270-EK2	ATA2270-EK2
ATAB5279	ATA5279	6-fold LF antenna driver	ATAB5279	ATAB5279	ATAB5279	ATAB5279
Mobile Parts with						
ATAB5753/54	ATA5753/54	RF transmitter for RKE				
ATAB5756/57	ATA5756/57	RF transmitter for TPMS				
ATAB5749	ATA5749	RF transmitter for RKE				
ATAB5811/12-RS	ATA5811	RF transceiver for remote start				
ATA5771/73/74-DK1	ATA5771/73/74	Tx-MCM				
ATA5795-EK1	ATA5795	for RKE incl. transponder function				
ATA5790-EK1	ATA5790 + TX ATA5749	for PEG using RF/LF-authentication link			ATA5790-EK1	ATA5790-EK1
ATA5790-3/-4-EK2	ATA5790 + TRX ATA5823/4	for PEG using RF/RF-authentication link	ATA5790-3-EK2	ATA5790-4-EK2		

Table 2. Complete Configuration for Passive Entry Go Applications

Car Infotainment

Radio

Car Antenna Amplifier Concepts

Stephan Gerlach

With the antenna driver IC ATR4251, Atmel provides a very successful solution for AM and FM antenna amplifiers. The device is mainly used in the cars radio's reception path facing challenging antenna types and reception positions within the car body. The ATR4251's advantages comprise high reliability and high functional density resulting in small design, maximum AC/DC parameter repeatability during production and long-time stability. The IC's high flexibility enables to meet the individual customer needs – especially in terms of cost and performance ratio.

As car design requirements more and more dominate technical aspects, however, the technical requirements for car antenna design also change. Since the amount of antennas in a medium- or luxury-class car easily reaches a number of 20 to 30, current antennas need to be almost invisible, or have at least a decent appearance. Consequently, antennas – especially those for radio and TV reception – tend to be integrated into the cars' windows. This is critical due to the limited window area, and also due to the fact that different antenna compete for the best window area position.

It is no surprise that the collected field strength results in a very low antenna voltage, which is even worse if loaded with the high capacitance of a long antenna cable. To avoid this, it is recommended to provide, for example in AM band, not only an LNA with an adjustable gain but also a buffer to drive long 50- or 75-Ohm cables.

Advantages of IC over Discrete Solutions

There are various advantages of antenna solutions using integrated circuits over discrete solutions, amongst others, stable operating point against temperature variation, component tolerances and aging, as well as a smaller design form factor which allows adding features that improve the technical performance but are too cost-expensive when realized as a discrete solution. Even if the amount of passive and active components within the integrated circuit exceeds those of a discrete solution, the stability and reliability of an IC-based solution is far beyond the discrete solution. This is due to the fact that each additional soldering connection is a potential failure root cause – especially in a car with its inherent long-lasting temperature, humidity and vibration test cycles.

However, only combined integrated technologies – e.g., BiCMOS as used in Atmel's integrated antenna amplifiers – can fully play its advantages over both discrete and simple integrated CMOS solutions. An AM antenna has a very high impedance and a fairly low capacitance, resulting in low antenna voltage. For such an antenna, an FET transistor with a low input capacitance is the preferred choice as first stage amplifier to match the antenna. It also needs to be taken into account that the high impedance and the far better noise/ linearity behaviour (compared to a bipolar transistor within the AM frequency band) allow to fully use the small signal from the antenna, and to handle large-signal reception conditions that might occur during driving.

The receiver probably needs a long coaxial cable that may cause a substantial loss due to its high inherent capacitance. The best way to overcome such a challenge is to attach a driver or buffer amplifier right before the cable. A smart biasing technique plus a push-pull circuit, comprising complementary

bipolar NPN and PNP transistors, perfectly matches the requirements and will maintain the high linearity performance of the entire amplifier chain.

To achieve best FM amplifier low-noise quality and easy input-output matching, a bipolar transistor is the best choice as GaAs or comparable solutions are too expensive in most cases.

A combination of different transistor types is useful for all other antenna amplifier features such as automatic gain control (AGC), voltage stabilization, plug detection, over-voltage and ESD protection.

For maximum linearity performance and best large-signal behaviour it is advantageous to use the entire battery voltage range, provided that a well-stabilized regulation is in place.

Most advanced CMOS technologies restrict the voltage swing more than necessary due to their inherent low breakthrough voltages. By using bipolar transistors, however, a maximum output voltage swing of up to 12 V_{pp} can be achieved at the output of the FM stage, resulting in excellent OIP3 (145 dBuV) and OIP2 (170 dBuV) values.

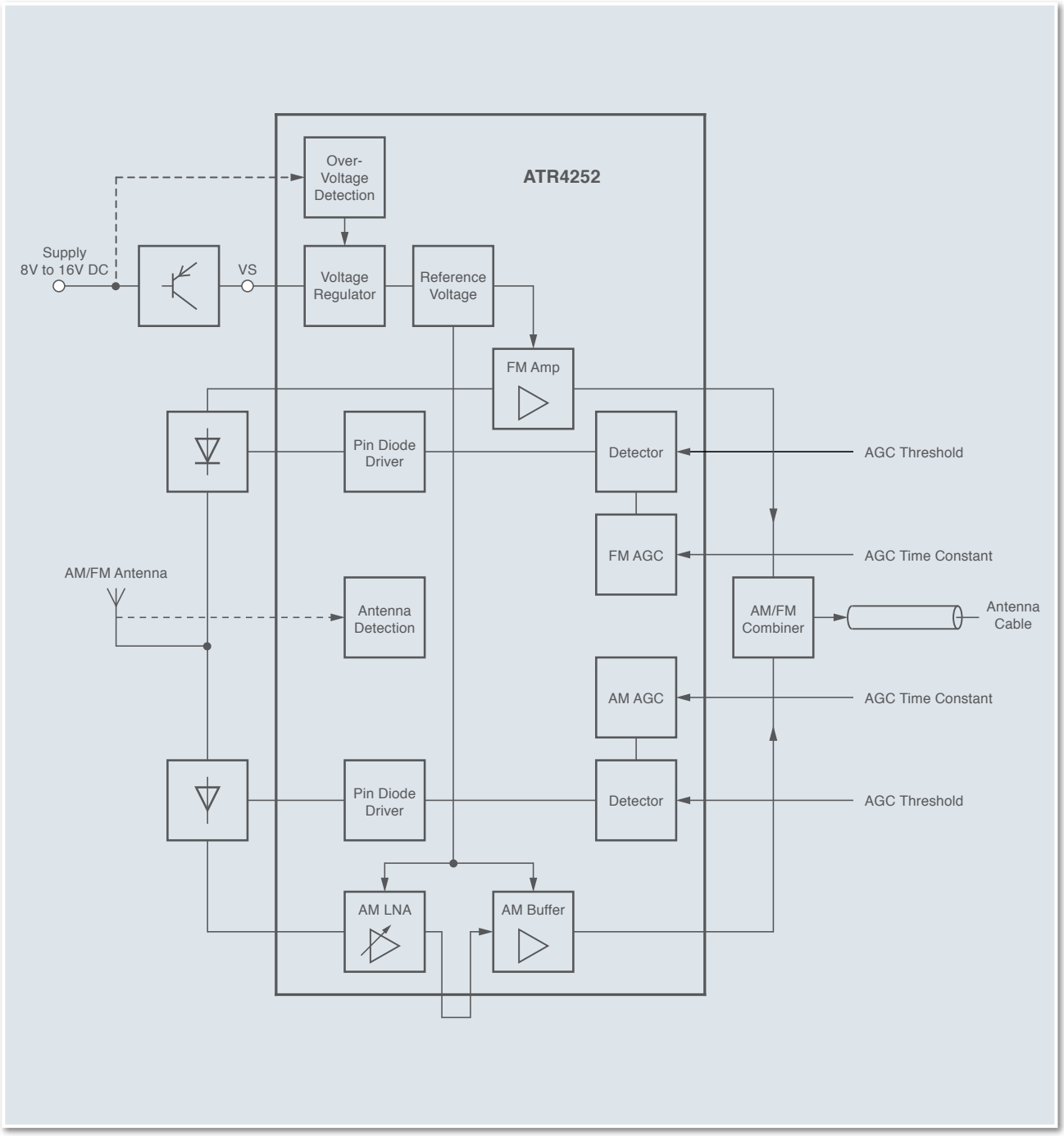

Figure 1. ATR4252 Block Diagram

For the functional block “AGC” it is also advantageous to use mixed circuitry, e.g., bipolar transistors as current sources for the PIN diode attenuators because bipolar transistors require less space than comparable MOS transistors for the same function.

Antenna Amplifier ATR4252

The ATR4252 is a further enhancement: it integrates even more external components, functional blocks and features, and the technical characteristics of the already existing blocks have been improved.

Performance Improvements

The ATR4252 provides outstanding noise level and linearity performance in both separate as well as combined AM and FM band amplifiers. The goal for the FM amplifier was to reduce the noise figure (NF) while maintaining the best possible intermodulation performance.

To perform this task, extensive simulations of the circuit, bond wires, package and external components were carried out. The achieved results for the common base configuration are shown in figure 2, which illustrates the noise figure comparison of final simulation run and measurement within the 80- to 170-MHz FM frequency band.

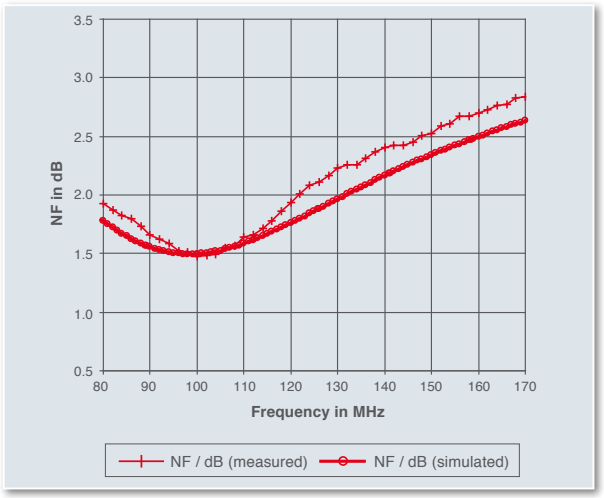

Figure 2. FM Amplifier Noise Figure

Thanks to proper current density, dedicated biasing techniques and further means, the achieved NF of 1.5 dB in FM is even better than results with dedicated discrete RF transistors, and matches well with the pre-running simulations.
When combining the AM and FM parts, however, it is inevitable to raise the FM noise figure at the combining point, depending on the required bandwidth of the AM amplifier part. If a maximum bandwidth of 30 MHz (especially for DRM reception) has to pass the low-pass filter of the combination point network, the noise figure will be about 1.9 dB. For the most common AM bandwidth of 450 kHz to 1.7 MHz, however, the increase is only 0.1 dB. This results in a final noise figure of about 1.6 dB, which is still a very good value.

If the designer wants to focus mainly on maximum linearity (more than 145 dBuV for OIP3) and less on the NF performance, this can easily be accomplished by adapting one external resistor placed at the emitter of the FM transistor.

A further reduction in BOM cost leads to the common emitter circuit that can also be realized using the ATR4252. The benefit of cost and board space reduction is accompanied with a slight reduction in noise and intermodulation performance.

AM Amplifier

One of the AM amplifier design goals was to provide a voltage gain of about 9 dB in addition to the insertion gain of the transimpedance amplifier used in ATR4251, while keeping the noise and intermodulation level on the same level as with ATR4251.
This has been achieved by using a monolithic combination of MOS and bipolar technology. The DC biasing of the relevant RF transistors, for example, has been optimized for best noise and intermodulation performance. Since the ATR4252 offers maximum modularity, it is possible to insert an external filter between LNA output and buffer input. Moreover, the voltage supply range has been extended to lower values (8V) without noticeable performance reduction.

In all other cases where this lower value is not needed, the ATR4252 provides a well stabilized and filtered supply voltage of 10V due to the integrated voltage stabilization circuit and one external PNP power transistor. This stabilization loop is able to suppress ripple and noise by more than 40 dB.

Overvoltage Protection and Antenna Detection

The antenna detection functionality is used to detect errors that may occur due to the following three main failure root causes:

1. A antenna plug that has not been fit properly during car production
2. A broken cable or a damaged reception structure of a printed glass antenna
3. A temporarily bad cable connection to antenna that is caused by vibrations/ movements of the car

The ATR4252 enables to set-up diagnostic system, which can be realized as an additional plug contact in the antenna-cable-amplifier chain or placed into the DC path of a window heating field in case the antenna is part of this structure.

This is possible because the integrated diagnostic system can both drive a current as well as detect a current that flows into the circuit. To realize one of the two possible placements in the heating structure (just below the 12V level or just above the GND level) it can detect a voltage window in the range of 0V to 3V, and 6V to 16V. The failure signalization to the car's diagnostic system is performed by a predefined DC current reduction of the complete antenna amplifier down to 20 mA.

Finally the overvoltage protection unit is able to reduce the overall current consumption of the complete IC to an innocuous value of 12 mA in case the applied DC voltage exceeds 16V.

Summary

Thanks to the device's outstanding technical features, the new integrated antenna amplifier ATR4252 enables to meet the car industry's highest performance and quality requirements. Its inbuilt flexibility allows creating one standard platform for the different car markets and antenna types, thus resulting in cost-efficient and durable products.

Ref.: 9020A-AUTO-10/09/03M